International Journal for Parasitology: Drugs and Drug Resistance 16 (2021) 45–64

Contents lists available at ScienceDirect

International Journal for Parasitology: Drugs and Drug Resistance

journal homepage: www.elsevier.com/locate/ijpddr

New diarylsulfonamide inhibitors of *Leishmania infantum* amastigotes

Myriam González [a,b,c], Pedro José Alcolea [d], Raquel Álvarez [a,b,c], Manuel Medarde [a,b,c], Vicente Larraga [d], Rafael Peláez [a,b,c,*]

[a] Laboratorio de Química Orgánica y Farmacéutica, Departamento de Ciencias Farmacéuticas, Facultad de Farmacia, Universidad de Salamanca, Salamanca, Spain
[b] Instituto de Investigación Biomédica de Salamanca (IBSAL), Facultad de Farmacia, Universidad de Salamanca, Salamanca, Spain
[c] Centro de Investigación de Enfermedades Tropicales de la Universidad de Salamanca (CIETUS), Facultad de Farmacia, Universidad de Salamanca, Salamanca, Spain
[d] Laboratorio de Parasitología Molecular, Departamento de Biología Celular y Molecular, Centro de Investigaciones Biológicas Margarita Salas, Consejo Superior de Investigaciones Científicas, Madrid, Spain

ARTICLE INFO

Keywords:
Leishmania
Amastigote
Sulfonamides
Tubulin

ABSTRACT

New drugs against visceral leishmaniasis with mechanisms of action differing from existing treatments and with adequate cost, stability, and properties are urgently needed. No antitubulin drug is currently in the clinic against *Leishmania infantum*, the causative agent of visceral leishmaniasis in the Mediterranean area. We have designed and synthesized a focused library of 350 compounds against the *Leishmania* tubulin based on the structure-activity relationship (SAR) and sequence differences between host and parasite. The compounds synthesized are accessible, stable, and appropriately soluble in water. We assayed the library against *Leishmania* promastigotes, axenic, and intracellular amastigotes and found 0, 8, and 16 active compounds, respectively, with a high success rate against intracellular amastigotes of over 10%, not including the cytotoxic compounds. Five compounds have a similar or better potency than the clinically used miltefosine. 14 compounds showed a host-dependent mechanism of action that might be advantageous as it may render them less susceptible to the development of drug resistance. The active compounds cluster in five chemical classes that provide structure-activity relationships for further hit improvement and facilitate series development. Molecular docking is consistent with the proposed mechanism of action, supported by the observed structure-activity relationships, and suggests a potential extension to other *Leishmania* species due to sequence similarities. A new family of diarylsulfonamides designed against the parasite tubulins is active against *Leishmania infantum* and represents a new class of potential drugs with favorable cost, stability, and aqueous solubility for the treatment of visceral leishmaniasis (VL). These results could be extended to other clinically relevant species of *Leishmania* spp.

1. Introduction

Leishmaniasis is a neglected tropical disease caused by protozoan parasites classified into the genus *Leishmania* (Kinetoplastida: Trypanosomatidae). The incidence is 700,000–2,000,000 cases causing 20,000–30,000 annual deaths (Alvar et al., 2012). The main clinical forms are kala-azar or visceral (VL), cutaneous (CL), and mucocutaneous leishmaniasis (MCL). VL is fatal without treatment. Anthroponotic VL (AVL) is caused by *Leishmania donovani* in Southeastern Asia and Western Africa, whereas *Leishmania infantum* causes zoonotic VL (ZVL) and distributes in the Mediterranean basin and South America. Dogs are the main reservoirs of ZVL, whose incidence is limited in humans in developed countries. Nevertheless, about a decade ago, an outbreak in humans was registered in Spain (Arce et al., 2013; Jiménez et al., 2014; Molina et al., 2012).

The life cycle of *Leishmania* spp. is digenetic and develops in two stages. The promastigote is a motile fusiform extracellular stage. The amastigote is a round intracellular stage whose flagellum does not emerge from the cellular body. Promastigotes undergo a differentiation process known as metacyclogenesis within the sand fly vector (Diptera: Psychodidae) gut. The vector injects highly infective metacyclic promastigotes in the mammalian host's dermis during blood feeding. Metacyclic promastigotes are internalized by phagocytes and differentiate into amastigotes. Amastigotes multiply within infected cells, affecting different tissues depending on the causative species. When a sand fly feeds on an infected host, amastigotes transform into procyclic

* Corresponding author. Laboratorio de Química Orgánica y Farmacéutica, Departamento de Ciencias Farmacéuticas, Facultad de Farmacia, Universidad de Salamanca, Salamanca, Spain.
E-mail address: pelaez@usal.es (R. Peláez).

https://doi.org/10.1016/j.ijpddr.2021.02.006
Received 13 October 2020; Received in revised form 22 February 2021; Accepted 22 February 2021
Available online 24 March 2021

promastigotes within the peritrophic membrane and begin differentiation into metacyclic forms as they migrate towards the anterior midgut (Alcolea et al., 2016; Escudero-Martínez et al., 2017).

The number of drugs available against the parasite is limited and they present toxicity, side effects, resistance (Jain and Jain, 2018), long-term treatment, and cost limitations [reviewed in (Nagle et al., 2014; Ponte-Sucre et al., 2017; Rama et al., 2015)]. Their efficacy varies depending on the species, the clinical development these species cause, and the host (Tiuman et al., 2011). Combination therapy of current treatments is being explored and slightlys improves (Zulfiqar et al., 2017). Hence, new drugs are required to control this challenging disease (Zhang et al., 2018). The most used drugs during the last 70 years have been pentavalent antimonials, administered by the intramuscular or the intravenous route. The long-term treatments cause serious side effects, including cardiac arrhythmia and acute pancreatitis (Monzote, 2009; Nagle et al., 2014). Resistance has decreased efficacy over time, which is related to multidrug resistance phenotypes (Légaré et al., 2001), mutations in the macrophage aquaporin AQP1 gene, and IL10-mediated up-regulation of the macrophage multiple resistance protein MDR1 (Marquis et al., 2005). Amphotericin B is a polyenic macrolide antibiotic with powerful antifungal and antileishmanial activity. This drug also causes several side effects, and is expensive, poorly soluble in water, not stable in the gastric environment, and poorly membrane permeable. Fungizone®, a micellar suspension of sodium deoxycholate, is administered by the intravenous route and the patients must be hospitalized and monitored (Abu Ammar et al., 2019; Monzote, 2009; Nagle et al., 2014). In the 1990s it replaced pentamidine as second-line therapy for refractory VL cases in India (Nagle et al., 2014). High-cost lipid formulations (AmBisome®) allow lower dosages and side effects, and help in VL control in the Indian subcontinent, but are ineffective against other species in other countries (De Rycker et al., 2018). Resistance has emerged associated with changes in ergosterol biosynthesis and oxidative stress prevention (Mbongo et al., 1998). Miltefosine was approved as a first-line drug in 2002 to replace antimonials in several regions (Nagle et al., 2014; Sundar et al., 2002). It initially showed significant antileishmanial activity, but a gradual increase in resistances related to transporters (Mondelaers et al., 2016; Pérez-Victoria et al, 2003, 2006) and relapses have followed (Rijal et al., 2013; Sundar and Murray, 2005). Paromomycin is efficacious as an ointment against CL but not frequently used due to its side effects, such as ototoxicity (Monzote, 2009; Sundar et al., 2007). Several drug classes, such as the aminopyrazoles, the nitroimidazoles, the oxaboroles, the proteasome inhibitors, and the kinase inhibitors, are currently in development against VL, but oral, safe, effective, low cost, and of short course administration new chemotypes acting on alternative targets are still required (Alves et al., 2018).

The sulfonamides are synthetically accessible, stable, drug-like compounds. They have a long history of clinical success (Drews, 2000). Their antiparasitic and antitumor effects are linked to inhibition of the microtubule dynamics (Dumontet and Jordan, 2010; Vicente-Blázquez et al., 2019). None of the current antileishmanial drugs in the clinical practice or clinical trials target tubulin. Diarylsulfonamides bind at the colchicine site of tubulin, inhibiting microtubule dynamics, and eliciting antimitotic activity (Vicente-Blázquez et al., 2019). They combine being a privileged scaffold for the generation of pharmacological activities with synthetic accessibility and adequate pharmacokinetic profiles, arising from a favorable combination of chemical stability, hydrogen bonding ability, polarity, hydrophilic-lipophilic balance, adjustable pK_a values, solubility, and conformational preferences (Laurence et al., 2009; Perlovich et al., 2014).

The microtubules of eukaryotic cells are made up of αβ-tubulin dimers, and most drugs affecting microtubule dynamics bind to tubulin dimer, microtubule lattice, or microtubule-associated proteins and motors. Tubulins are highly conserved throughout evolution. However, differences between the mammalian and parasitic orthologs suggest sufficient binding selectivity for drug development. These cytoskeletal supramolecular structures are involved in structural support, cell motility, cell division, organelle transport, maintenance of cell morphology, and signal transduction (Jordan et al., 1998). Specifically, *Leishmania* tubulin is an essential component of the flagellum and the subpellicular microtubules. These structures are related to parasite survival (Sinclair and de Graffenried, 2019; Sunter and Gull, 2017). At least seven drug-binding sites have been identified in tubulin and the microtubules, named after their prototypical drugs: the taxanes, the Vinca minor alkaloids, the maytansine, the peloruside/laulimalide, the eribulin, the pironetin, and the colchicine binding sites (Vicente-Blázquez et al., 2019). Different parasitic species show sequence variations compared to their hosts which vary depending on the sites, thus making them more or less susceptible to specific drug classes and representatives, thus allowing for specific treatments (Dostál and Libusová, 2014). *Leishmania* parasites are not susceptible to colchicine (Luis et al., 2013), the archetypical ligand of the mammalian eponymous domain. Hence, an opportunity for selective ligand development arises like in the treatment of helminth and fungal parasitosis with antimitotic benzimidazoles binding at the colchicine site, such as triclabendazole or albendazole (Lacey, 1990).

2. Materials and methods

2.1. Chemical synthesis

2.1.1. General chemical techniques

Reagents were used as purchased without further purification. Solvents (EtOAc, DMF, CH_2Cl_2, toluene, MeOH and CH_3CN) were stored over molecular sieves. THF was refluxed with sodium/benzophenone and hexane was dried by distillation and stored over $CaCl_2$. TLC was performed on precoated silica gel polyester plates (0.25 mm thickness) with a UV fluorescence indicator 254 (Polychrom SI F254). Chromatographic separations were performed on silica gel columns by flash (Kieselgel 40, 0.040–0.063; Merck) chromatography. Melting points were determined on a Buchi 510 apparatus and are uncorrected. ^{1}H NMR and ^{13}C NMR spectra were recorded in $CDCl_3$, CD_3OD, DMSO-D_6 or Acetone-D_6 on a Bruker WP 200-SY spectrometer at 200/50 MHz or a Bruker SY spectrometer at 400/100 MHz. Chemical shifts (δ) are given in ppm downfield from tetramethylsilane and coupling constants (*J* values) are in Hertz. IR spectra were run on a Nicolet Impact 410 Spectrophotometer. A hybrid QSTAR XL quadrupole/time of flight spectrometer was used for HRMS analyses. GC-MS spectra were performed using a Hewlett-Packard 5890 series II mass detector. A Helios-α UV-320 from Thermo-Spectronic was used for UV spectra.

2.1.2. 1,4-Dimethoxy-2-nitrobenzene (74)

To a solution of 1,4-dimethoxybenzene (2.35 g, 17 mmol) in acetic acid (30 mL) at 0 °C, nitric acid (1.13 mL, 17 mmol) in acetic acid (20 mL) was added dropwise under nitrogen atmosphere. The reaction mixture was stirred at 0 °C for 4 h and then poured onto ice with 5% $NaHCO_3$ and extracted with ethyl acetate. The organic layers were washed to neutrality with brine, dried over anhydrous Na_2SO_4, filtered and concentrated in vacuum to obtain 2.92 g (94%) of **74**. M.p.: 71.8–72.5 °C (CH_2Cl_2/Hexane). IR (KBr): 1528, 874, 763 cm^{-1}. ^{1}H NMR (400 MHz, $CDCl_3$): δ 3.82 (3H, *s*), 3.92 (3H, *s*), 7.03 (1H, *d*, $J = 9.6$), 7.12 (1H, *dd*, $J = 9.6$ and 3.2), 7.4 (1H, *d*, $J = 3.2$). ^{13}C NMR (100 MHz, $CDCl_3$): δ 55.9 (CH_3), 56.9 (CH_3), 109.9 (CH), 115.0 (CH), 120.8 (CH), 139.3 (C), 147.3 (C), 152.7 (C). GC-MS ($C_8H_9NO_4$): 183 (M^+).

2.1.3. 2,5-Dimethoxyaniline (75)

1,4-dimethoxy-2-nitrobenzene (**74**, 2.92 g, 15.95 mmol) was suspended in ethyl acetate (100 mL) and was palladium-catalyzed (Pd (C) 10 mg) reduced under H_2 atmosphere for 48 h. The reaction mixture was filtered through Celite® and the solvent evaporated in vacuum to isolate 2.42 g (99%) of **75**. Crude reaction product was obtained and used without further purification. IR (KBr): 3459, 1519, 839 cm^{-1}. ^{1}H NMR

(400 MHz, $CDCl_3$): δ 3.72 (3H, *s*), 3.79 (3H, *s*), 6.24 (1H, *dd*, $J = 9.2$ and 3.2), 6.33 (1H, *d*, $J = 3.2$), 6.69 (1H, *d*, $J = 9.2$). ^{13}C NMR (100 MHz, $CDCl_3$): δ 54.5 (CH_3), 55.1 (CH_3), 100.9 (CH), 101.1 (CH), 110.3 (CH), 136.2 (C), 140.9 (C), 153.3 (C). GC-MS ($C_8H_{11}NO_2$): 153 (M^+).

2.1.4. N-(2,5-dimethoxyphenyl)-4-methoxybenzenesulfonamide (76)

To a solution of **75** (2.42 g, 15.84 mmol) in CH_2Cl_2 (50 mL) and pyridine (2 mL), was slowly added 4-methoxybenzenesulfonyl chloride (3.27 g, 15.84 mmol). The mixture was stirred at room temperature for 4 h. Then the reaction was treated with 2N HCl and 5% $NaHCO_3$, washed with brine, dried over anhydrous Na_2SO_4 and the solvent evaporated to obtain 4.9 g (95%) of **76**. It was purified by crystallization in CH_2Cl_2/Hexane (4.29 g, 84%). M.p.: 114–115 °C (CH_2Cl_2/Hexane). IR (KBr): 3313, 1578, 830 cm^{-1}. ^1H NMR (400 MHz, $CDCl_3$): δ 3.62 (3H, *s*), 3.74 (3H, *s*), 3.81 (3H, *s*), 6.53 (1H, *dd*, $J = 9.2$ and 3.2), 6.65 (1H, *d*, $J = 9.2$), 6.86 (2H, *d*, $J = 9.2$), 7.01 (1H, *s*), 7.14 (1H, *d*, $J = 3.2$), 7.72 (2H, *d*, $J = 9.2$). ^{13}C NMR (100 MHz, $CDCl_3$): δ 55.5 (CH_3), 55.7 (CH_3), 56.2 (CH_3), 106.8 (CH), 109.5 (CH), 111.4 (CH), 113.9 (2CH), 126.8 (C), 129.4 (2CH), 130.7 (C), 143.4 (C), 153.8 (C), 163.0 (C). HRMS ($C_{15}H_{17}NO_5S + H^+$): calcd 324.0900 ($M + H^+$), found 324.0900.

2.1.5. N-(2,5-dimethoxy-4-nitrophenyl)-4-methoxybenzenesulfonamide (96)

To a stirred solution at 0 °C of **76** (2.07 g, 6.42 mmol) in acetic acid (30 mL), nitric acid (0.44 mL, 6.42 mmol) in acetic acid (20 mL) was slowly added under nitrogen atmosphere. After 4 h at 0 °C, the reaction mixture was poured onto ice and basified with 5% $NaHCO_3$ solution. Then it was extracted with ethyl acetate. The organic layers were washed with brine, dried over anhydrous Na_2SO_4, filtered and concentrated in vacuum to obtain 2.14 g (90%) of **96**. By crystallization in CH_2Cl_2/Hexane 1.53 g (65%) of purified product were isolated. M.p.: 161–163 °C (CH_2Cl_2/Hexane). IR (KBr): 3277, 1522, 1450, 822 cm^{-1}. ^1H NMR (400 MHz, $CDCl_3$): δ 3.76 (3H, *s*), 3.79 (3H, *s*), 3.88 (3H, *s*), 6.9 (2H, *d*, $J = 9.2$), 7.26 (1H, *s*), 7.39 (1H, *s*), 7.56 (1H, *s*), 7.77 (2H, *d*, $J = 9.2$). ^{13}C NMR (100 MHz, $CDCl_3$): δ 55.7 (CH_3), 56.6 (CH_3), 57.0 (CH_3), 103.2 (CH), 108.3 (CH), 114.4 (2CH), 129.4 (2CH), 129.9 (C), 132.8 (C), 133.1 (C), 141.1 (C), 149.2 (C), 163.6 (C). HRMS ($C_{15}H_{16}N_2O_7S + H^+$): calcd 369.0751 ($M + H^+$), found 369.0753.

2.1.6. N-(4-amino-2,5-dimethoxyphenyl)-4-methoxybenzenesulfonamide (104)

The nitro sulfonamide **96** (1.44 g, 3.91 mmol) in ethyl acetate (100 mL) and Pd (C) (10 mg) was stirred at room temperature under H_2 atmosphere for 48 h. By filtration through Celite® and solvent evaporation, hydrogenated sulfonamide **104** (1.28 g, 97%) was obtained. 1.11 g (84%) of **104** were isolated by crystallization in CH_2Cl_2/Hexane. M.p.: 164–166 °C (CH_2Cl_2/Hexane). IR (KBr): 3430, 3291, 1451, 834 cm^{-1}. ^1H NMR (400 MHz, $CDCl_3$): δ 3.38 (3H, *s*), 3.79 (3H, *s*), 3.82 (3H, *s*), 6.15 (1H, *s*), 6.54 (1H, *s*), 6.82 (2H, *d*, $J = 9.2$), 7.04 (1H, *s*), 7.58 (2H, *d*, $J = 9.2$). ^{13}C NMR (100 MHz, $CDCl_3$): δ 55.5 (CH_3), 55.9 (CH_3), 56.2 (CH_3), 99.2 (CH), 108.4 (CH), 113.5 (2CH), 115.3 (C), 129.4 (2CH), 130.7 (C), 134.6 (C), 141.0 (C), 145.8 (C), 162.7 (C). HRMS ($C_{15}H_{18}N_2O_5S + H^+$): calcd 339.1009 ($M + H^+$), found 339.1012.

2.1.7. 2-Chloro-N-(2,5-dimethoxy-4-((4-methoxyphenyl)sulfonamido) phenyl)acetamide (129)

To a solution of amine **104** (160 mg, 0.47 mmol) in CH_2Cl_2 (25 mL) 2-chloroacetyl chloride (46.4 μL, 0.57 mmol) was added dropwise under nitrogen atmosphere. After 12 h at room temperature the reaction was washed with water, dried over anhydrous Na_2SO_4 and the solvent evaporated in vacuum to give 171 mg (87%) of **129.** The crude reaction product was purified by crystallization in methanol (55 mg, 28%). M.p.: 175–177 °C (MeOH). IR (KBr): 3372, 3265, 1677, 1598, 829 cm^{-1}. ^1H NMR (400 MHz, CD_3OD): δ 3.47 (3H, *s*), 3.81 (3H, *s*), 3.86 (3H, *s*), 4.25 (2H, *s*), 6.94 (2H, *d*, $J = 8.8$), 7.14 (1H, *s*), 7.62 (2H, *d*, $J = 8.8$), 7.74 (1H, *s*). ^{13}C NMR (100 MHz, Acetone-D_6): δ 43.2 (CH_2), 55.1 (CH_3), 55.8 (CH_3), 56.0 (CH_3), 104.1 (CH), 106.9 (CH), 113.8 (2CH), 124.8 (C), 129.3 (2CH), 131.4 (C), 138.1 (C), 142.4 (C), 144.9 (C), 163.0 (C), 164.1 (C). HRMS ($C_{17}H_{19}ClN_2O_6S + H^+$): calcd 415.0725 ($M + H^+$), found 415.0700.

2.1.8. 3-Chloro-N-(2,5-dimethoxy-4-((4-methoxyphenyl)sulfonamido) phenyl)propanamide (138)

To a stirred solution at room temperature of **104** (143 mg, 0.42 mmol) in CH_2Cl_2 (30 mL) 3-chloropropanoyl chloride (49.4 μL, 0.51 mmol) was slowly added under nitrogen atmosphere. After 12 h, the reaction mixture was crystallized in CH_2Cl_2 to obtain 88 mg (48%) of **138**. M.p.: 193–197 °C (CH_2Cl_2). ^1H NMR (400 MHz, CD_3OD): δ 2.89 (2H, *t*, $J = 6.4$), 3.47 (3H, *s*), 3.81 (3H, *s*), 3.83 (3H, *s*), 3.83 (2H, *t*, $J = 6.4$), 6.95 (2H, *d*, $J = 9.2$), 7.12 (1H, *s*), 7.63 (2H, *d*, $J = 9.2$), 7.68 (1H, *s*). ^{13}C NMR (100 MHz, Acetone-D_6): δ 39.6 (CH_2), 40.1 (CH_2), 55.1 (CH_3), 55.7 (CH_3), 55.9 (CH_3), 104.4 (CH), 107.1 (CH), 113.7 (2CH), 120.9 (C), 125.7 (C), 129.3 (2CH), 131.7 (C), 142.2 (C), 144.9 (C), 162.9 (C), 167.8 (C). HRMS ($C_{18}H_{21}ClN_2O_6S + H^+$): calcd 429.0882 ($M + H^+$), found 429.0879.

2.1.9. 4-Methoxy-3-nitrobenzonitrile (250)

To a solution of 4-methoxy-3-nitrobenzaldehyde (870 mg, 4.80 mmol) in MeOH (30 mL) hydroxylamine hydrochloride (334 mg, 4.80 mmol) and two drops of pyridine were added. After 24 h at reflux, the solvent was evaporated, the obtained residue was dissolved in CH_2Cl_2 and washed with water, dried over anhydrous Na_2SO_4, evaporated under vacuum, and dissolved in 15 mL of pyridine. Finally, acetic anhydride (1 mL) was added to the mixture. After 9 h at room temperature, the reaction was treated with 2N HCl, extracted with CH_2Cl_2 and the solvent evaporated to obtain 685 mg (80%) of **250**. Crude reaction product was obtained and used without further purification. ^1H NMR (400 MHz, $CDCl_3$): δ 4.05 (3H, *s*), 7.20 (1H, *d*, $J = 8.8$), 7.83 (1H, *dd*, $J = 8.8$ and 2), 8.15 (1H, *d*, $J = 2$). GC-MS ($C_8H_6N_2O_3$): 178 (M^+).

2.1.10. 3-Amino-4-methoxybenzonitrile (258)

To a solution of **250** (685 mg, 3.84 mmol) in ethyl acetate (100 mL) Pd (C) (10 mg) was added and the reaction was stirred at room temperature under H_2 atmosphere for 48 h. By filtration through Celite® and solvent evaporation, 529 mg (93%) of crude reaction **258** was obtained and used without further purification.^1H NMR (400 MHz, $CDCl_3$): δ 3.83 (3H, *s*), 6.71 (1H, *d*, $J = 8$), 6.84 (1H, *d*, $J = 2$), 6.87 (1H, *s*), 6.98 (1H, *dd*, $J = 8$ and 2). GC-MS ($C_8H_8N_2O$): 148 (M^+).

2.1.11. N-(5-cyano-2-methoxyphenyl)-4-methoxybenzenesulfonamide (276A) and 4-cyano-2-((4-methoxyphenyl)sulfonamido)phenyl 4-methoxybenzenesulfonate (276B)

To a solution of **258** (529 mg, 3.57 mmol) in CH_2Cl_2 (50 mL) and pyridine (2 mL) 4-methoxybenzenesulfonyl chloride (1.106 g, 5.35 mmol) was slowly added. The mixture was stirred at room temperature for 4 h. Then the reaction was treated with 2N HCl and 5% $NaHCO_3$, washed with brine, dried over anhydrous Na_2SO_4 and the solvent evaporated in vacuum to give a residue that was purified by silica gel chromatography using hexane/EtOAc (7:3) to yield the sulfonamides **276A** (466 mg, 41%) and **276B** (205 mg, 30%). **276A:** ^1H NMR (400 MHz, $CDCl_3$): δ 3.80 (3H, *s*), 3.83 (3H, *s*), 6.80 (1H, *d*, $J = 8$), 6.91 (2H, *d*, $J = 9.2$), 7.09 (1H, *s*), 7.33 (1H, *dd*, $J = 8$ and 2), 7.75 (2H, *d*, $J = 9.2$), 7.76 (1H, *d*, $J = 2$). ^{13}C NMR (100 MHz, $CDCl_3$): δ 55.6 (CH_3), 56.1 (CH_3), 104.5 (C), 110.9 (CH), 114.2 (2CH), 118.6 (C), 122.6 (CH), 127.2 (C), 129.4 (2CH), 129.5 (CH), 130.1 (C), 152.1 (C), 163.4 (C). HRMS ($C_{15}H_{14}N_2O_4S + Na^+$): calcd 341.0569 ($M + Na^+$), found 341.0566. **276B:** IR (KBr): 2233, 1462, 833, 749 cm^{-1}. ^1H NMR (400 MHz, $CDCl_3$): δ 3.83 (3H, *s*), 3.91 (3H, *s*), 6.91 (2H, *d*, $J = 9.2$), 7.01 (2H, *d*, $J = 8.8$), 7.03 (1H, *d*, $J = 8$), 7.15 (1H, *s*), 7.25 (1H, *dd*, $J = 8$ and 2), 7.73 (2H, *d*, $J = 9.2$), 7.75 (2H, *d*, $J = 8.8$), 7.78 (1H, *d*, $J = 2$). ^{13}C NMR (100 MHz, $CDCl_3$): δ 55.6 (CH_3), 55.9 (CH_3), 111.5 (C), 114.5 (2CH), 115.0 (2CH), 117.4 (C), 123.7 (CH), 124.4 (CH), 124.8 (C), 128.4 (CH), 129.4 (2CH),

129.8 (C), 130.8 (2CH), 131.5 (C), 142.4 (C), 163.6 (C), 165.1 (C). HRMS ($C_{21}H_{18}N_2O_7S_2$ + Na^+): calcd 497.0448 (M + Na^+), found 497.0409.

2.1.12. 4-Methoxy-3-nitrobenzenesulfonyl chloride (86)

To a stirred solution at 0 °C of 4-methoxybenzenesulfonyl chloride (4.41 g, 21.36 mmol) in CH_2Cl_2 (20 mL) and H_2SO_4 (5 mL) nitric acid (0.95 mL, 21.36 mmol) was dropwise added under nitrogen atmosphere. After 4 h, the reaction was poured onto ice and the mixture was kept at 4 °C for 30 min. Then, the precipitate was filtered under vacuum to dryness to obtain 4.97 g (92%) of **86**. ^{1}H NMR (400 MHz, $CDCl_3$): δ 4.11 (3H, *s*), 7.33 (1H, *d, J* = 8.8), 8.20 (1H, *dd, J* = 8.8 and 2.4), 8.48 (1H, *d, J* = 2.4). ^{13}C NMR (100 MHz, $CDCl_3$): δ 57.0 (CH_3), 114.0 (CH), 124.8 (CH), 127.1 (C), 132.2 (CH), 135.0 (C), 157.1 (C). GC-MS ($C_7H_6ClNO_5S$): 251 (M^+).

2.1.13. N-(2,5-dimethoxyphenyl)-4-methoxy-3-nitrobenzenesulfonamide (183)

To 650 mg of the amine **75** (4.24 mmol) in CH_2Cl_2 (50 mL) and pyridine (2 mL), 1.07 g (4.24 mmol) of the sulfonyl chloride **86** was slowly added and stirred at room temperature for 6 h. The reaction was treated with 2N HCl and 5% $NaHCO_3$, washed with brine, dried over anhydrous Na_2SO_4 and the solvent evaporated to obtain 4.9 g (95%) of **76**. The residue was crystallized in CH_2Cl_2/Hexane to afford the purified compound (4.29 g, 84%). M.p.: 121–123 °C (CH_2Cl_2/Hexane). ^{1}H NMR (400 MHz, $CDCl_3$): δ 3.61 (3H, *s*), 3.72 (3H, *s*), 3.96 (3H, *s*), 6.56 (1H, *dd, J* = 8.8 and 3.2), 6.65 (1H, *d, J* = 8.8), 7.07 (1H, *d, J* = 8.8), 7.09 (1H, *d, J* = 3.2), 7.16 (1H, *s*), 7.88 (1H, *dd, J* = 8.8 and 2.4), 8.22 (1H, *d, J* = 2.4). ^{13}C NMR (100 MHz, $CDCl_3$): δ 55.7 (CH_3), 56.0 (CH_3), 57.0 (CH_3), 108.1 (CH), 110.5 (CH), 111.4 (CH), 113.6 (CH), 125.2 (CH), 125.5 (C), 130.9 (C), 133.1 (CH), 138.8 (C), 143.9 (C), 153.8 (C), 155.8 (C). HRMS ($C_{15}H_{16}N_2O_7S$ + Na^+): calcd 391.0563 (M + Na^+), found 391.0570.

2.1.14. N-(4-bromo-2,5-dimethoxyphenyl)-4-methoxy-N-methyl-3-nitrobenzenesulfonamide (204)

To a stirred solution of **183** (86 mg, 0.23 mmol) in CH_2Cl_2 (25 mL) *N*-bromosuccinimide (41 mg, 0.23 mmol) was added. After 2 h the solvent was evaporated in vacuum and the residue was re-dissolved in CH_3CN. 25 mg of crushed KOH (0.36 mmol) and 17 μL of methyl iodide (0.27 mmol) were added to the reaction mixture and it was stirred at room temperature for 24 h. Finally, it was concentrated, re-dissolved in CH_2Cl_2, washed with brine, dried over anhydrous Na_2SO_4, filtered and concentrated in vacuum. The residue was purified by silica gel chromatography using toluene/EtOAc (8:2) to afford 87 mg (80%) of **204**. ^{1}H NMR (400 MHz, $CDCl_3$): δ 3.18 (3H, *s*), 3.43 (3H, *s*), 3.88 (3H, *s*) 4.01 (3H, *s*), 6.96 (1H, *s*), 6.99 (1H, *d, J* = 9.2), 7.01 (1H, *s*), 7.68 (1H, *dd, J* = 9.2 and 2.4), 7.72 (1H, *d, J* = 2.4). ^{13}C NMR (100 MHz, $CDCl_3$): δ 37.7 (CH_3), 55.5 (CH_3), 56.6 (CH_3), 56.9 (CH_3), 111.0 (CH), 112.0 (C), 116.1 (CH), 116.6 (CH), 127.2 (CH), 127.9 (C), 130.2 (CH), 131.6 (C), 139.0 (C), 149.9 (C), 150.0 (C), 157.6 (C). HRMS ($C_{16}H_{17}BrN_2O_7S$ + H^+): calcd 462.9877 (M + H^+), found 462.9992.

2.1.15. N-(2,5-dimethoxyphenyl)-4-nitrobenzenesulfonamide (130)

To a solution of **75** (1.06 g, 6.89 mmol) in CH_2Cl_2 (50 mL) and pyridine (2 mL) was slowly added 4-nitrobenzenesulfonyl chloride (1.53 g, 6.89 mmol). The mixture was stirred at room temperature for 4 h. Then the reaction was treated with 2N HCl and 5% $NaHCO_3$, washed with brine, dried over anhydrous Na_2SO_4 and the solvent evaporated to obtain 2.09 g (90%) of the sulfonamide **130**. The crude reaction product was purified by crystallization in CH_2Cl_2/Hexane (1.274 g, 55%). M.p.: 164–168 °C (CH_2Cl_2/Hexane). ^{1}H NMR (400 MHz, $CDCl_3$): δ 3.57 (3H, *s*), 3.74 (3H, *s*), 6.58 (1H, *dd, J* = 9.2 and 2.8), 6.65 (1H, *d, J* = 9.2), 7.15 (1H, *d, J* = 2.8), 7.93 (2H, *d, J* = 9.2), 8.22 (2H, *d, J* = 9.2). ^{13}C NMR (100 MHz, $CDCl_3$): δ 55.8 (CH_3), 56.0 (CH_3), 108.3 (CH), 110.6 (CH), 111.5 (CH), 123.9 (2CH), 125.3 (C), 128.5 (2CH), 143.8 (C), 144.7 (C), 150.1 (C), 153.8 (C). HRMS ($C_{14}H_{14}N_2O_6S$ + Na^+): calcd 361.0465 (M + Na^+), found 361.0463.

2.1.16. N-(4-bromo-2,5-dimethoxyphenyl)-4-nitrobenzenesulfonamide (296)

To a stirred solution of **130** (1.95 g, 5.76 mmol) in CH_2Cl_2 (100 mL) *N*-bromosuccinimide (1.23 g, 6.92 mmol) was added. After 4 h at room temperature the reaction was washed with water, dried over anhydrous Na_2SO_4 and the solvent evaporated in vacuum to give 2.35 g (98%) of **296.** The crude reaction product was purified by crystallization in methanol (1.26 g, 52%). M.p.: 190–196 °C (MeOH). ^{1}H NMR (400 MHz, $CDCl_3$): δ 3.57 (3H, *s*), 3.88 (3H, *s*), 6.94 (1H, *s*), 6.97 (1H, *s*), 7.24 (1H, *s*), 7.90 (2H, *d, J* = 8.8), 8.27 (2H, *d, J* = 8.8). ^{13}C NMR (100 MHz, $CDCl_3$): δ 56.8 (CH_3), 57.5 (CH_3), 107.6 (CH), 108.7 (C), 116.6 (CH), 124.6 (2CH), 124.8 (C), 129.0 (2CH), 144.7 (C), 145.1 (C), 150.8 (C), 151.0 (C). HRMS ($C_{14}H_{13}BrN_2O_6S$ + Na^+): calcd 438.9580 and 440.9561 (M + Na^+), found 438.9570 and 440.9549.

2.1.17. 4-Amino-N-(4-bromo-2,5-dimethoxyphenyl)benzenesulfonamide (302)

To an EtOH/HOAc/H_2O mixture (2:2:1, 12.5 mL) HCl (c) (1 drop), **296** (2.35 g, 5.63 mmol) and Fe (3.15 g, 56.3 mmol) were added and the reaction stirred for 2 h at 100 °C. After extraction with CH_2Cl_2, filtration through Celite® and treatment with 5% $NaHCO_3$, the crude reaction mixture was purified by silica gel chromatography using hexane/EtOAc (7:3) to yield 1.02 g (47%) of **302.** IR (KBr): 3368, 1498, 822 cm^{-1}. ^{1}H NMR (400 MHz, CD_3OD): δ 3.55 (3H, *s*), 3.77 (3H, *s*), 6.57 (2H, *d, J* = 8.8), 7.00 (1H, *s*), 7.11 (1H, *s*), 7.39 (2H, *d, J* = 8.8). ^{13}C NMR (100 MHz, Acetone-d_6): δ 56.2 (CH_3), 56.3 (CH_3), 105.0 (C), 105.9 (CH), 112.9 (2CH), 116.3 (CH), 125.6 (C), 127.4 (C), 129.3 (2CH), 144.5 (C), 150.1 (C), 152.9 (C). HRMS ($C_{14}H_{15}BrN_2O_4S$ + Na^+): calcd 408.9828 and 410.9808 (M + Na^+), found 408.9825 and 410.9793.

2.1.18. N-(4-(N-(4-bromo-2,5-dimethoxyphenyl)sulfamoyl)phenyl) formamide (315)

690 mg of **302** (1.78 mmol) were dissolved in CH_2Cl_2 (70 mL), pyridine (5 mL) and formic acid (10 mL) and stirred at room temperature. After 24 h, the reaction mixture was poured onto ice and treated with 2N HCl and 5% $NaHCO_3$. The organic layers were washed to neutrality with brine, dried over anhydrous Na_2SO_4, filtered and evaporated to dryness to afford 708 mg (95%) of **315**. The crude reaction product was purified by crystallization in methanol (307 mg, 41%). M.p.: 202–207 °C (MeOH). IR (KBr): 3337, 1702, 1593, 831 cm^{-1}. ^{1}H NMR (400 MHz, CD_3OD): δ 3.49 (3H, *s*), 3.81 (3H, *s*), 7.01 (1H, *s*), 7.15 (1H, *s*), 7.67 (4H, *bs*), 8.30 (1H, *s*). ^{13}C NMR (100 MHz, DMSO-d_6): δ 56.9 (CH_3), 57.0 (CH_3), 107.1 (C), 109.8 (CH), 117.1 (CH), 119.1 (2CH), 126.2 (C), 128.6 (2CH), 134.8 (C), 142.8 (C), 146.9 (C), 149.6 (C), 160.6 (CH). HRMS ($C_{15}H_{14}BrN_2O_5S$ + Na^+): calcd 436.9777 and 438.9757 (M + Na^+), found 436.9772 and 438.9750.

2.1.19. N-(4-bromo-2,5-dimethoxyphenyl)-4-(methylamino) benzenesulfonamide (323)

To a solution of the formamide **315** (680 mg, 1.64 mmol) and $NaBH_4$ (93 mg, 2.45 mmol) in dry THF (15 mL) at 0 °C, trichloroacetic acid (401 mg, 2.45 mmol) in dry THF (10 mL) was added dropwise under nitrogen atmosphere. The reaction mixture was stirred at 0 °C to room temperature for 24 h and then concentrated and re-dissolved in EtOAc, washed with brine, dried over anhydrous Na_2SO_4, filtered and solvent evaporated in vacuum. The residue was purified by silica gel chromatography using hexane/EtOAc (8:2) to yield 246 mg (37%) of **323**. IR (KBr): 3420, 3251, 1599, 820 cm^{-1}. ^{1}H NMR (400 MHz, CD_3OD): δ 2.76 (3H, *s*), 3.56 (3H, *s*), 3,78 (3H, *s*), 6.51 (2H, *d, J* = 8.8), 7.00 (1H, *s*), 7.13 (1H, *s*), 7,45 (2H, *d, J* = 8.8). ^{13}C NMR (100 MHz, $CDCl_3$): δ 30.0 (CH_3), 56.5 (CH_3), 56.8 (CH_3), 105.3 (CH), 105.5 (C), 111.1 (2CH), 115.8 (CH), 125.0 (C), 126.6 (C), 129.3 (2CH), 143.5 (C), 150.2 (C), 152.7 (C). HRMS ($C_{15}H_{16}BrN_2O_4S$ + Na^+): calcd 422.9985 and 424.9964 (M + Na^+), found 422.9985 and 424.9959.

*2.1.20. N-benzyl-N-(4-bromo-2,5-dimethoxyphenyl)-4-(methylamino) benzenesulfonamide (**332**)*

35 mg (0.25 mmol) of K_2CO_3 were added to a stirred solution of **323** (50 mg, 0.12 mmol) in 3 mL of dry DMF. After 1 h at room temperature 21.7 μL (0.19 mmol) of benzyl chloride were added and stirred for 24 h. The reaction mixture was concentrated, re-dissolved in CH_2Cl_2, washed with brine, dried over anhydrous Na_2SO_4, filtered and concentrated in vacuum to obtain 59 mg (96%) and crystallized in MeOH (23 mg, 38%). M.p.: 177–183 °C (MeOH). ^{1}H NMR (400 MHz, $CDCl_3$): δ 2.79 (3H, *s*), 3.33 (3H, *s*), 3.57 (3H, *s*), 4.64 (2H, *s*), 6.46 (2H, *d, J* = 8.8), 6.52 (1H, *s*), 6.85 (1H, *s*), 7.14 (5H, *m*), 7.44 (2H, *d, J* = 8.8). ^{13}C NMR (100 MHz, $CDCl_3$): δ 30.1 (CH_3), 53.3 (CH_2), 55.7 (CH_3), 56.7 (CH_3), 110.8 (2CH), 111.5 (C), 116.5 (CH), 117.5 (CH), 126.5 (C), 126.9 (C), 127.4 (CH), 128.2 (2CH), 128.7 (2CH), 129.7 (2CH), 136.7 (C), 149.4 (C), 151.0 (C), 152.4 (C). HRMS ($C_{22}H_{23}BrN_2O_4S$ + Na^+): calcd 515.0415 (M + Na^+), found 515.0434.

*2.1.21. 3,4,5-Trimethoxy-2-((4-methoxyphenyl)sulfonamido)benzoic acid (63A) and 3,4,5-trimethoxy-2-(3,4,5-trimethoxy-2-((4-methoxyphenyl) sulfonamido)benzamido)benzoic acid (**63B**)*

To a stirred solution of 2-amino-3,4,5-trimethoxybenzoic acid (300 mg, 1.32 mmol) in CH_2Cl_2 (50 mL) and pyridine (2 mL) 4-methoxybenzenesulfonyl chloride (273 g, 1.32 mmol) was slowly added. After 6 h, the reaction mixture was poured onto a 2N HCl solution and extracted with CH_2Cl_2. The organic layers were washed to neutrality with saturated NaCl, dried over anhydrous Na_2SO_4, filtered and evaporated to dryness. The residue was purified by two successive crystallizations in CH_2Cl_2/hexane, compounds **63A** (40 mg, 8%) and **63B** (17 mg, 4%) were isolated. **63A:** M.p.: 165–167 °C (CH_2Cl_2/Hexane). IR (KBr): 3264, 2939, 1668, 1458, 837 cm^{-1}. ^{1}H NMR (400 MHz, $CDCl_3$): δ 3.45 (3H, *s*), 3.84 (3H, *s*), 3.88 (3H, *s*), 3.91 (3H, *s*), 6.93 (2H, *d, J* = 8.8), 7.28 (1H, *s*), 7.77 (2H, *d, J* = 8.8), 8.7 (1H, *s*). ^{13}C NMR (100 MHz, $CDCl_3$): δ 55.6 (CH_3), 56.1 (CH_3), 60.3 (CH_3), 61.1 (CH_3), 109.0 (CH), 113.7 (2CH), 116.5 (C), 128.0 (C), 129.4 (2CH), 132.0 (C), 147.7 (C), 148.4 (C), 150.5 (C), 162.8 (C), 171.4 (C). HRMS ($C_{17}H_{19}NO_8S$ + H^+): calcd 398.0901 (M + H^+), found 398.0905. **63B:** M.p.: 170–171 °C (CH_2Cl_2/Hexane). ^{1}H NMR (400 MHz, $CDCl_3$): δ 3.35 (3H, *s*), 3.75 (3H, *s*), 3.79 (3H, *s*), 3.84 (3H, *s*), 3.88 (3H, *s*), 3.96 (3H, *s*), 3.99 (3H, *s*), 6.85 (2H, *d, J* = 8.8), 7.20 (1H, *s*), 7.25 (1H, *s*), 7.68 (2H, *d, J* = 8.8), 8.15 (1H, *s*), 9.22 (1H, *s*). ^{13}C NMR (100 MHz, $CDCl_3$): δ 57.1 (CH_3), 59.0 ($2CH_3$), 61.9 (CH_3), 62.4 (CH_3), 62.6 (CH_3), 63.0 (CH_3), 108.9 (CH), 110.2 (CH), 115.2 (2CH), 120.9 (C), 124.1 (C), 126.6 (C), 127.4 (C), 131.3 (2CH), 133.2 (C), 147.0 (C), 148.3 (C), 149.7 (C), 149.9 (C), 152.9 (C), 153.4 (C), 153.9 (C), 165.3 (C), 167.5 (C). HRMS ($C_{27}H_{30}N_2O_{12}S$ + H^+): calcd 607.1599 (M + H^+), found 607.1593.

*2.1.22. N-(3,5-dimethoxyphenyl)-4-methoxybenzenesulfonamide (**259**)*

To a solution of 3,5-dimethoxyaniline (290 mg, 1.89 mmol) in CH_2Cl_2 (50 mL) and pyridine (2 mL), was slowly added 4-methoxybenzenesulfonyl chloride (469 mg, 2.27 mmol). The mixture was stirred at room temperature for 4 h. Then the reaction was treated with 2N HCl and 5% $NaHCO_3$, washed with brine, dried over anhydrous Na_2SO_4 and the solvent evaporated to obtain 596 mg (97%) of the sulfonamide **259**. The crude reaction product was purified by crystallization in CH_2Cl_2/Hexane (438 mg, 71%). M.p.: 115–122 °C (CH_2Cl_2/Hexane). IR (KBr): 3234, 1595, 824 cm^{-1}. ^{1}H NMR (400 MHz, $CDCl_3$): δ 3.66 (6H, *s*), 3.77 (3H, *s*), 6.13 (1H, *t, J* = 2), 6.17 (2H, *d, J* = 2), 6.85 (2H, *d, J* = 8.8), 7.68 (2H, *d, J* = 8.8). ^{13}C NMR (100 MHz, $CDCl_3$): δ 55.3 ($2CH_3$), 55.5 (CH_3), 97.0 (CH), 98.9 (2CH), 114.2 (2CH), 129.5 (2CH), 130.4 (C), 138.6 (C), 161.1 (2C), 163.1 (C). HRMS ($C_{15}H_{17}NO_5S$ + H^+): calcd 324.0909 (M + H^+), found 324.0900.

*2.1.23. N-benzyl-N-(3,5-dimethoxyphenyl)-4-methoxybenzenesulfonamide (**270**)*

To a stirred solution of **259** (90 mg, 0.28 mmol) in dry DMF (3 mL) 78 mg (0.56 mmol) of K_2CO_3 was added. After 1 h at room temperature, 48.5 μL (0.42 mmol) of benzyl chloride was added and stirred for 24 h. The reaction mixture was concentrated, re-dissolved in CH_2Cl_2, washed with brine, dried over anhydrous Na_2SO_4, filtered and concentrated under vacuum to produce 104 mg (90%) of crude reaction product from which 81 mg (70%) of **270** were purified by crystallization. M.p.: 146–150 °C (MeOH). IR (KBr): 3467, 1458, 806 cm^{-1}. ^{1}H NMR (400 MHz, $CDCl_3$): δ 3.62 (6H, *s*), 3.87 (3H, *s*), 4.65 (2H, *s*), 6.12 (2H, *d, J* = 2), 6.28 (1H, *t, J* = 2), 6.94 (2H, *d, J* = 8.8), 7.22 (5H, *m*), 7.63 (2H, *d, J* = 8.8). ^{13}C NMR (100 MHz, $CDCl_3$): δ 54.7 (CH_2), 55.3 ($2CH_3$), 55.6 (CH_3), 100.0 (CH), 107.2 (2CH), 113.9 (2CH), 127.5 (CH), 128.3 (2CH), 128.5 (2CH), 129.8 (2CH), 130.3 (C), 136.1 (C), 140.9 (C), 160.4 (2C), 162.9 (C). HRMS ($C_{22}H_{23}NO_5S$ + H^+): calcd 414.1370 (M + H^+), found 414.1369.

*2.1.24. N-benzyl-N-(4-bromo-3,5-dimethoxyphenyl)-4-methoxybenzenesulfonamide (**326A**), N-benzyl-N-(2-bromo-3,5-dimethoxyphenyl)-4-methoxybenzenesulfonamide (**326B**) and N-benzyl-N-(2,4-dibromo-3,5-dimethoxyphenyl)-4-methoxybenzenesulfonamide (**326C**)*

To a solution of **270** (195 mg, 0.47 mmol) in CH_2Cl_2 (40 mL) *N*-bromosuccinimide (168 mg, 0.94 mmol) was added and stirred for 48 h at room temperature. After that, the reaction was washed with water, dried over anhydrous Na_2SO_4 and the solvent evaporated in vacuum to produce 183 mg. The residue was flash chromatographed on silica gel (hexane/EtOAc 8:2) to afford the purified compounds: **326A** (116 mg, 50%), **326B** (24 mg, 10%) and **326C** (6 mg, 2%). **326A:** M.p.: 199–203 °C (MeOH). IR (KBr): 3435, 1589, 836 cm^{-1}. ^{1}H NMR (200 MHz, $CDCl_3$): δ 3.65 (6H, *s*), 3.88 (3H, *s*), 4.68 (2H, *s*), 6.12 (2H, *s*), 6.97 (2H, *d, J* = 9), 7.22 (5H, *bs*), 7.65 (2H, *d, J* = 9). ^{13}C NMR (100 MHz, $CDCl_3$): δ 54.9 (CH_2), 55.7 (CH_3), 56.4 ($2CH_3$), 100.5 (C), 105.8 (2CH), 114.0 (2CH), 127.8 (CH), 128.4 (2CH), 128.6 (2CH), 129.9 (C), 130.0 (2CH), 135.7 (C), 139.4 (C), 156.7 (2C), 163.1 (C). HRMS ($C_{22}H_{22}BrNO_5S$ + H^+): calcd 492.0475 and 494.0454 (M + H^+), found 492.0473 and 494.0440. **326B:** IR (KBr): 2938, 1593, 831 cm^{-1}. ^{1}H NMR (200 MHz, $CDCl_3$): δ 3.57 (3H, *s*), 3.80 (3H, *s*), 3.87 (3H, *s*), 4.60 (1H, *d, J* = 14.4), 4.89 (1H, *d, J* = 14.4), 6.14 (1H, *d, J* = 2.8), 6.38 (1H, *d, J* = 2.8), 6.94 (2H, *d, J* = 9), 7.20 (5H, *bs*), 7.74 (2H, *d, J* = 9). ^{13}C NMR (100 MHz, $CDCl_3$): δ 54.4 (CH_2), 55.5 (CH_3), 55.6 (CH_3), 56.3 (CH_3), 100.0 (CH), 105.9 (C), 109.4 (CH), 113.9 (2CH), 127.7 (CH), 128.2 (2CH), 129.4 (2CH), 130.1 (2CH), 131.8 (C), 135.7 (C), 138.8 (C), 157.2 (C), 158.9 (C), 163.0 (C). HRMS ($C_{22}H_{22}BrNO_5S$ + H^+): calcd 492.0475 and 494.0454 (M + H^+), found 492.0467 and 494.0447. **326C:** IR (KBr): 2935, 1595, 835 cm^{-1}. ^{1}H NMR (200 MHz, $CDCl_3$): δ 3.60 (3H, *s*), 3.77 (3H, *s*), 3.87 (3H, *s*), 4.55 (1H, *d, J* = 14.4), 4.97 (1H, *d, J* = 14.4), 6.30 (1H, *s*), 6.95 (2H, *d, J* = 9), 7.22 (5H, *m*), 7.73 (2H, *d, J* = 9). ^{13}C NMR (100 MHz, $CDCl_3$): δ 54.2 (CH_2), 55.6 (CH_3), 56.5 (CH_3), 60.5 (CH_3), 108.8 (C), 112.4 (C), 112.8 (CH), 114.0 (2CH), 128.0 (CH), 128.3 (2CH), 129.4 (2CH), 130.0 (2CH), 131.5 (C), 135.4 (C), 137.4 (C), 155.6 (C), 155.7 (C), 163.2 (C). HRMS ($C_{22}H_{21}Br_2NO_5S$ + H): calcd 569.9580 and 571.9559 (M^+ + H), found 569.9577 and 571.9558.

*2.1.25. N-(3,5-dimethoxyphenyl)-4-nitrobenzenesulfonamide (**242**)*

To a solution of 3,5-dimethoxyaniline (1.39 g, 9.98 mmol) in CH_2Cl_2 (50 mL) and pyridine (2 mL), was slowly added 4-nitrobenzenesulfonyl chloride (2.21 g, 9.07 mmol) and stirred at room temperature for 12 h. Then the reaction mixture was treated with 2N HCl and 5% $NaHCO_3$. The organic layers were washed to neutrality with brine, dried over anhydrous Na_2SO_4 and concentrated under vacuum to yield 2.66 g (87%) of the sulfonamide **242**. The crude reaction product was purified by crystallization in CH_2Cl_2/Hexane (2.43 g, 79%). M.p.: 131–139 °C (CH_2Cl_2/Hexane). ^{1}H NMR (400 MHz, $CDCl_3$): δ 3.71 (6H, *s*), 6.22 (1H, *t, J* = 2.4), 6.25 (2H, *d, J* = 2.4), 7.98 (2H, *d, J* = 8.8), 8.28 (2H, *d, J* = 8.8). ^{13}C NMR (100 MHz, $CDCl_3$): δ 55.4 ($2CH_3$), 97.4 (CH), 99.7 (2CH), 124.3 (2CH), 128.6 (2CH), 137.4 (C), 144.4 (C), 150.1 (C), 161.3 (2C). HRMS ($C_{14}H_{14}N_2O_6S$ + H^+): calcd 339.0653 (M + H^+), found 339.0645.

*2.1.26. 4-Amino-N-(3,5-dimethoxyphenyl)benzenesulfonamide (**245**)*

To a solution of **242** (2.60 g, 7.69 mmol) in ethyl acetate (150 mL) and MeOH (5 mL), Pd (C) (10 mg) was added and the reaction was stirred at room temperature under H_2 atmosphere for 24 h. By filtration through Celite® and solvent evaporation, 2.30 g (97%) of **245** was obtained and purified by crystallization in MeOH (1.53 g, 65%). M.p.: 149–155 °C (MeOH). IR (KBr): 3450, 3370, 1458, 821 cm^{-1}. ^1H NMR (400 MHz, CD_3OD): δ 3.67 (6H, *s*), 6.13 (1H, *t, J* = 2.4), 6.25 (2H, *d, J* = 2.4), 6.60 (2H, *d, J* = 8.8), 7.46 (2H, *d, J* = 8.8). ^{13}C NMR (100 MHz, CD_3OD): δ 54.2 ($2CH_3$), 95.6 (CH), 98.2 (2CH), 112.8 (2CH), 125.3 (C), 128.8 (2CH), 139.8 (C), 152.8 (C), 161.1 (2C). HRMS ($C_{14}H_{16}N_2O_4S$ + H^+): calcd 309.0904 (M + H^+), found 309.0915.

*2.1.27. N-(3,5-dimethoxyphenyl)-4-(dimethylamino)benzenesulfonamide (**254**)*

To a solution of *p*-formaldehyde (534 mg, 17.77 mmol) in MeOH (40 mL), 548 mg of **245** (1.77 mmol) were added and stirred for 30 min, then $NaBH_3CN$ (223 mg, 10.62 mmol) was added and the reaction was heated at reflux for 24 h. The reaction mixture was concentrated, poured onto ice and extracted with EtOAc, dried over Na_2SO_4, filtered through Celite® and the solvent evaporated in vacuum to afford 580 mg (97%) of **254**. M.p.: 158–164 °C (MeOH). IR (KBr): 3228, 1498, 812 cm^{-1}. ^1H NMR (400 MHz, CD_3OD): δ 2.99 (6H, *s*), 3.67 (6H, *s*), 6.12 (1H, *t, J* = 2.4), 6.26 (2H, *d, J* = 2.4), 6.68 (2H, *d, J* = 9.2), 7.58 (2H, *d, J* = 9.2). ^{13}C NMR (100 MHz, $CDCl_3$): δ 39.9 ($2CH_3$), 55.3 ($2CH_3$), 96.6 (CH), 98.4 (2CH), 110.8 (2CH), 123.9 (C), 129.1 (2CH), 139.1 (C), 152.9 (C), 161.1 (2C). HRMS ($C_{16}H_{20}N_2O_4S$ + H^+): calcd 337.1217 (M + H^+), found 337.1205.

*2.1.28. N-benzyl-N-(3,5-dimethoxyphenyl)-4-(dimethylamino) benzenesulfonamide (**275**)*

77 mg (0.55 mmol) of K_2CO_3 were added to a stirred solution of **254** (93 mg, 0.27 mmol) in 3 mL of dry DMF. After 1 h at room temperature 48.2 μL (0.41 mmol) of benzyl chloride were added and stirred for 24 h. The reaction mixture was concentrated, re-dissolved in EtOAc, washed with brine, dried over anhydrous Na_2SO_4, filtered and concentrated in vacuum to obtain 112 mg (95%) and crystallized in MeOH (62 mg, 52%). M.p.: 155–160 °C (MeOH). IR (KBr): 3471, 1455, 811 cm^{-1}. ^1H NMR (400 MHz, $CDCl_3$): δ 3.05 (6H, *s*), 3.63 (6H, *s*), 4.63 (2H, *s*), 6.18 (2H, *d, J* = 2.4), 6.26 (1H, *t*, J = 2.4), 6.64 (2H, *d, J* = 8.8), 7.20 (5H, *m*), 7.53 (2H, *d, J* = 8.8). ^{13}C NMR (100 MHz, $CDCl_3$): δ 40.1 ($2CH_3$), 54.5 (CH_2), 55.3 ($2CH_3$), 99.9 (CH), 107.1 (2CH), 110.6 (2CH), 123.9 (C), 127.4 (CH), 128.2 (2CH), 128.5 (2CH), 129.6 (2CH), 136.4 (C), 141.4 (C), 152.8 (C), 160.3 (2C). HRMS ($C_{23}H_{26}N_2O_4S$ + H^+): calcd 427.1686 (M + H^+), found 427.1658.

*2.1.29. N-(6-methoxypyridin-3-yl)-4-nitrobenzenesulfonamide (**283**)*

To a solution of 6-methoxypyridin-3-amine (1.82 g, 14.66 mmol) in CH_2Cl_2 (50 mL) and pyridine (2 mL), was slowly added 4-nitrobenzenesulfonyl chloride (3.9 g, 17.59 mmol). The mixture was stirred at room temperature for 4 h. Then the reaction was treated with 2N HCl and 5% $NaHCO_3$, washed with brine, dried over anhydrous Na_2SO_4 and the solvent evaporated to obtain 3.10 g (68%) of **273**. It was purified by crystallization in MeOH 2.67 g (59%). M.p.: 139–143 °C (MeOH). IR (KBr): 3208, 1610, 1350, 826 cm^{-1}. ^1H NMR (400 MHz, $CDCl_3$): δ 3.88 (3H, *s*), 6.49 (1H, *s*), 6.70 (1H, *d, J* = 8.8), 7.43 (1H, *dd, J* = 8.8 and 2.8), 7.72 (1H, *d, J* = 2.8), 7.88 (2H, *d, J* = 9.2), 8.31 (2H, *d, J* = 9.2). ^{13}C NMR (100 MHz, $CDCl_3$): δ 53.8 (CH_3), 111.5 (CH), 124.4 (2CH), 125.2 (C), 128.6 (2CH), 136.3 (CH), 143.2 (CH), 144.3 (C), 150.3 (C), 163.1 (C). HRMS ($C_{12}H_{11}N_3O_5S$ + H^+): calcd 310.0492 (M + H^+), found 310.0487.

*2.1.30. 4-Amino-N-(6-methoxypyridin-3-yl)benzenesulfonamide (**287**)*

3.00 g of **283** (9.71 mmol) was suspended in ethyl acetate (120 mL) and was palladium-catalyzed (Pd (C) 10 mg) reduced under H_2 atmosphere for 72 h. The reaction mixture was filtered through Celite® and the solvent evaporated in vacuum to isolate 2.67 g (98%) of **287**. Crude reaction product was purified by crystallization in MeOH (539 mg, 20%). M.p.: 176–180 °C (MeOH). IR (KBr): 3485, 3281, 1619, 1500, 794 cm^{-1}. ^1H NMR (400 MHz, CD_3OD): δ 3.82 (3H, *s*), 6.59 (2H, *d, J* = 8.4), 6.68 (1H, *d, J* = 8.8), 7.33 (2H, *d, J* = 8.4), 7.41 (1H, *dd, J* = 8.8 and 2.4), 7.71 (1H, *d, J* = 2.4). ^{13}C NMR (100 MHz, CD_3OD): δ 52.7 (CH_3), 110.1 (CH), 112.8 (2CH), 124.6 (C), 128.4 (C), 128.8 (2CH), 135.2 (CH), 141.2 (CH), 152.9 (C), 161.9 (C). HRMS ($C_{12}H_{13}N_3O_5S$ + H^+): calcd 280.0750 (M + H^+), found 280.0745.

*2.1.31. N-(4-(N-(6-methoxypyridin-3-yl)sulfamoyl)phenyl)formamide (**309**)*

970 mg of **287** (3.57 mmol) were dissolved in CH_2Cl_2 (100 mL), pyridine (5 mL) and formic acid (15 mL) and stirred at room temperature. After 24 h, the reaction mixture was poured onto ice and treated with 2N HCl and 5% $NaHCO_3$. The organic layers were washed to neutrality with brine, dried over anhydrous Na_2SO_4, filtered and evaporated to dryness to afford 555 mg (52%) of **309**. The crude reaction product was purified by crystallization in methanol (368 mg, 34%). M.p.: 189–193 °C (MeOH). IR (KBr): 3349, 3273, 1698, 1592, 823 cm^{-1}. ^1H NMR (400 MHz, CD_3OD): δ 3.82 (3H, *s*), 6.69 (1H, *d, J* = 8.8), 7.42 (1H, *dd, J* = 8.8 and 2.8), 7.62 (2H, *d, J* = 8.8), 7.70 (2H, *d, J* = 8.8), 7.71 (1H, *d, J* = 2.8), 8.31 (1H, *s*). ^{13}C NMR (100 MHz, Acetone-D6): δ 52.8 (CH_3), 110.6 (CH), 118.9 (2CH), 128.0 (C), 128.4 (2CH), 133.9 (C), 134.8 (CH), 141.6 (CH), 142.3 (C), 159.6 (C), 161.9 (CH). HRMS ($C_{13}H_{13}N_3O_4S$ + H^+): calcd 308.0703 (M + H^+), found 308.0700.

*2.1.32. N-(6-methoxypyridin-3-yl)-4-(methylamino)benzenesulfonamide (**316**)*

To a solution of the formamide **309** (485 mg, 1.58 mmol) and $NaBH_4$ (90 mg, 2.37 mmol) in dry THF (15 mL) at 0 °C, trichloroacetic acid (387 mg, 2.37 mmol) in dry THF (10 mL) was added dropwise under nitrogen atmosphere. The reaction mixture was stirred at 0 °C to room temperature for 24 h and then concentrated and re-dissolved in EtOAc, washed with brine, dried over anhydrous Na_2SO_4, filtered and solvent evaporated in vacuum. The crude reaction product (334 mg, 72%) was purified by crystallization in MeOH to yield 137 mg (30%) of **316**. M.p.: 183–186 °C (MeOH). IR (KBr): 3387, 3277, 1500, 821 cm^{-1}. ^1H NMR (400 MHz, CD_3OD): δ 2.76 (3H, *s*), 3.82 (3H, *s*), 6.52 (2H, *d, J* = 8.8), 6.67 (1H, *d, J* = 8.8), 7.38 (2H, *d, J* = 8.8), 7.41 (1H, *dd, J* = 8.8 and 2.8), 7.71 (1H, *d, J* = 2.8). ^{13}C NMR (100 MHz, $CDCl_3$): δ 30.0 (CH_3), 53.6 (CH_3), 111.0 (CH), 111.3 (2CH), 124.8 (C), 127.0 (C), 129.3 (2CH), 135.9 (CH), 142.5 (CH), 152.7 (C), 162.4 (C). HRMS ($C_{13}H_{15}N_3O_3S$ + H^+): calcd 294.0907 (M + H^+), found 294.0907.

*2.1.33. N-(4-(N-(6-methoxypyridin-3-yl)sulfamoyl)phenyl)-N-methylformamide (**320**)*

The compound **316** (88 mg, 0.30 mmol) was stirred in a mixture of CH_2Cl_2 (50 mL), pyridine (2 mL) and formic acid (5 mL) at room temperature for 24 h. The reaction mixture was poured onto ice and treated with 2N HCl and 5% $NaHCO_3$, washed to neutrality with brine, dried over anhydrous Na_2SO_4, filtered and solvent evaporated to produce 33 mg (34%) of **320**, which crystallized in methanol (24 mg, 25%). M.p.: 164–172 °C (MeOH). ^1H NMR (400 MHz, CD_3OD): δ 3.30 (3H, *s*), 3.82 (3H, *s*), 6.69 (1H, *d, J* = 8.8), 7.44 (2H, *d, J* = 8.8), 7.46 (1H, *dd, J* = 8.8 and 2.8), 7.71 (1H, *d, J* = 2.8), 7.74 (2H, *d, J* = 8.8), 8.65 (1H, *s*). ^{13}C NMR (100 MHz, CD_3OD): δ 29.9 (CH_3), 52.8 (CH_3), 110.7 (CH), 120.2 (2CH), 127.9 (C), 128.6 (2CH), 134.8 (CH), 135.6 (C), 141.5 (CH), 146.3 (C), 161.4 (C), 161.9 (CH). HRMS ($C_{14}H_{15}N_3O_4S$ + H^+): calcd 322.0856 (M + H^+), found 322.0855.

*2.1.34. 4-Methoxy-N-(6-methoxypyridin-3-yl)benzenesulfonamide (**240**)*

To a stirred solution of 6-methoxypyridin-3-amine (312 mg, 2.51 mmol) in CH_2Cl_2 (25 mL) and pyridine (1 mL) 4-methoxybenzenesulfonyl chloride (623 mg, 3.02 mmol) was added under nitrogen atmosphere. After 6 h, the reaction mixture was treated with 2N HCl and 5%

$NaHCO_3$ solutions. The organic layers were washed to neutrality with saturated NaCl, dried over anhydrous Na_2SO_4, filtered and evaporated to yield 631 mg (85%) of the sulfonamide **240**. The residue was purified by flash chromatography on silica gel using hexane/EtOAc (6:4) to afford 464 mg (62%). ^{1}H NMR (400 MHz, $CDCl_3$): δ 3.80 (3H, *s*), 3.83 (3H, *s*), 6.62 (1H, *d, J* = 8.8), 6.87 (2H, *d, J* = 8.8), 7.40 (1H, *dd, J* = 8.8 and 2.8), 7.63 (2H, *d, J* = 8.8), 7.75 (1H, *d, J* = 2.8). ^{13}C NMR (100 MHz, $CDCl_3$): δ 54.3 (CH_3), 56.2 (CH_3), 111.6 (CH) 114.9 (2CH), 127.5 (C), 130.1 (2CH), 130.6 (C), 136.3 (CH), 143.1 (CH), 162.9 (C), 163.8 (C). HRMS ($C_{13}H_{14}N_2O_4S + H^+$): calcd 295.0747 ($M + H^+$), found 295.0761.

2.1.35. N-benzyl-4-methoxy-N-(6-methoxypyridin-3-yl) benzenesulfonamide (279)

92 mg (0.31 mmol) of **240** dissolved in dry DMF (3 mL) were stirred for 1 h in the presence of K_2CO_3 (97 mg, 0.62 mmol). After that, benzyl chloride (54.5 μL 0.47 mmol) was added and stirred for 24 h. The reaction mixture was concentrated, re-dissolved in EtOAc, washed with brine, dried over anhydrous Na_2SO_4, filtered and concentrated in vacuum to obtain 112 mg (93%) and crystallized in MeOH (77 mg, 64%). M.p.: 144–146 °C (MeOH). IR (KBr): 3435, 1490, 823 cm^{-1}. ^{1}H NMR (400 MHz, CD_3OD): δ 3.81 (3H, *s*), 3.89 (3H, *s*), 4.72 (2H, *s*), 6.61 (1H, *d, J* = 8.8), 7.10 (2H, *d, J* = 8.8), 7.22 (5H, *bs*), 7.23 (1H, *dd, J* = 8.8 and 2.8), 7.62 (2H, *d, J* = 8.8), 7.67 (1H, *d, J* = 2.8). ^{13}C NMR (100 MHz, $CDCl_3$): δ 53.7 (CH_3), 54.9 (CH_2), 55.7 (CH_3), 110.8 (CH), 114.2 (2CH), 127.8 (CH), 128.5 (2CH), 128.6 (2CH), 129.2 (C), 129.7 (2CH), 130.7 (C), 135.4 (C), 139.5 (CH), 147.2 (CH), 163.0 (C), 163.1 (C). HRMS ($C_{20}H_{20}N_2O_4S + H^+$): calcd 385.1217 ($M + H^+$), found 385.1210.

2.1.36. N-(3,4-dimethoxyphenyl)-4-methoxybenzenesulfonamide (8)

To 2.49 g of 3,4-dimethoxyaniline (16.26 mmol) in CH_2Cl_2 (50 mL) and pyridine (4 mL), 3.61 g of 4-methoxybenzenesulfonyl chloride was slowly added (16.26 mmol) and stirred at room temperature for 12 h. The reaction was treated with 2N HCl and 5% $NaHCO_3$, washed with brine, dried over anhydrous Na_2SO_4 and the solvent evaporated to obtain 5.29 g (99%) of **8**. The residue was crystallized in CH_2Cl_2/Hexane to afford the purified compound (4.04 g, 75%). M.p.: 101–102 °C (CH_2Cl_2/Hexane). IR (KBr): 3224, 1498, 801 cm^{-1}. ^{1}H NMR (400 MHz, $CDCl_3$): δ 3.75 (3H, *s*), 3.79 (3H, *s*), 3.80 (3H, *s*), 6.53 (1H, *dd, J* = 8.8 and 2.8), 6.66 (1H, *d, J* = 8.8), 6.70 (1H, *d, J* = 2.8), 6.86 (2H, *d, J* = 8.8), 7.66 (2H, *d, J* = 8.8). ^{13}C NMR (100 MHz, $CDCl_3$): δ 55.5 (CH_3), 55.9 (CH_3), 55.9(CH_3), 107.7 (CH), 111.1 (CH), 114.0 (2CH), 115.4 (CH), 129.4 (2CH), 129.5 (C), 130.3 (C), 147.2 (C), 149.1 (C), 163.0 (C). HRMS ($C_{15}H_{17}NO_5S + H^+$): calcd 324.0900 ($M + H^+$), found 324.0906.

2.1.37. N-(4,5-dimethoxy-2-nitrophenyl)-4-methoxybenzenesulfonamide (11)

To a solution of **8** (588 mg, 1.82 mmol) in CH_3CN (50 mL) *tert*-butyl nitrite (120 μL, 0.91 mmol) was added and stirred at 45 °C. After 1 h, additional 0.91 mmol *tert*-butyl nitrite was added to the reaction mixture and it was stirred at 45 °C for 24 h. The mixture was poured onto ice and basified with 5% $NaHCO_3$ solution and extracted with EtOAc. The organic layers were washed with brine, dried over Na_2SO_4 and concentrated under vacuum to yield **11** (638 mg, 95%). The residue was purified by crystallization in CH_2Cl_2/Hexane to afford 527 mg (78%). M.p.: 152–154 °C (CH_2Cl_2/Hexane). IR (KBr): 3257, 1521, 1499, 804 cm^{-1}. ^{1}H NMR (400 MHz, $CDCl_3$): δ 3.83 (3H, *s*), 3.87 (3H, *s*), 3.98 (3H, *s*), 6.90 (2H, *d, J* = 9.2), 7.35 (1H, *s*), 7.53 (1H, *s*), 7.73 (2H, *d, J* = 9.2). ^{13}C NMR (100 MHz, $CDCl_3$): δ 55.7 (CH_3), 56.3 (CH_3), 56.7 (CH_3), 103.0 (CH), 107.2 (CH), 114.4 (2CH), 129.4 (2CH), 129.7 (C), 129.9 (C), 130.3 (C), 145.2 (C), 155.4 (C), 163.6 (C). HRMS ($C_{15}H_{16}N_2O_7S + H^+$): calcd 369.0751 ($M + H^+$), found 369.0752.

2.1.38. N-(2-amino-4,5-dimethoxyphenyl)-4-methoxybenzenesulfonamide (12)

To a solution of **11** (620 mg, 1.68 mmol) in ethyl acetate (100 mL) Pd (C) (10 mg) was added and the reaction was stirred at room temperature under H_2 atmosphere for 48 h. By filtration through Celite® and solvent evaporation, 550 mg (96%) of crude **12** was obtained. 374 mg (65%) of the purified compound were isolated by crystallization in CH_2Cl_2/Hexane. M.p.: 102–112 °C (CH_2Cl_2/Hexane). IR (KBr): 3265, 1458, 835 cm^{-1}. ^{1}H NMR (400 MHz, $CDCl_3$): δ 3.46 (3H, *s*), 3.74 (3H, *s*), 3.79 (3H, *s*), 5.72 (1H, *s*), 5.88 (1H, *s*), 6.23 (1H, *s*), 6.87 (2H, *d, J* = 8.4), 7.61 (2H, *d, J* = 8.4). ^{13}C NMR (100 MHz, $CDCl_3$): δ 55.6 (CH_3), 55.8 (CH_3), 56.2 (CH_3), 101.0 (CH), 112.4 (C), 112.9 (CH), 114.1 (2CH), 129.8 (2CH), 130.4 (C), 139.0 (C), 141.5 (C), 149.6 (C), 163.1 (C). HRMS ($C_{15}H_{18}N_2O_5S + H^+$): calcd 339.1009 ($M + H^+$), found 339.1018.

2.1.39. N-(2-amino-4,5-dimethoxyphenyl)-4-methoxy-N-methylbenzenesulfonamide (120)

To a solution of **12** (167 mg, 0.49 mmol) in CH_3CN (25 mL) 68 mg of crushed KOH (0.98 mmol) and 62 μL of methyl iodide (0.98 mmol) were added and stirred at room temperature for 24 h. Then, the reaction mixture was concentrated, re-dissolved in CH_2Cl_2, washed with brine, dried over anhydrous Na_2SO_4, filtered and concentrated in vacuum to produce 140 mg (80%) of **120**. The crude reaction product was purified by crystallization in MeOH (52 mg, 30%). M.p.: 140–141 °C (MeOH). ^{1}H NMR (400 MHz, $CDCl_3$): δ 3.11 (3H, *s*), 3.46 (3H, *s*), 3.82 (3H, *s*), 3.87 (3H, *s*), 5.80 (1H, *s*), 6.34 (1H, *s*), 6.97 (2H, *d, J* = 8.8), 7.65 (2H, *d, J* = 8.8). ^{13}C NMR (100 MHz, $CDCl_3$): δ 40.2 (CH_3), 56.9 (CH_3), 57.0 (CH_3), 57.6 (CH_3), 101.9 (CH), 112.1 (CH), 115.2 (2CH), 119.4 (C), 129.8 (C), 131.6 (2CH), 141.5 (C), 142.2 (C), 151.1 (C), 164.4 (C). HRMS ($C_{16}H_{20}N_2O_5S + H^+$): calcd 353.1166 ($M + H^+$), found 353.1179.

2.1.40. N-(4,5-dimethoxy-2-((4-methoxy-N-methylphenyl)sulfonamido) phenyl)acetamide (124)

90 mg of **120** (0.25 mmol) was dissolved in CH_2Cl_2 (45 mL) and pyridine (1 mL). 29 μL of acetic anhydride (0.30 mmol) was added to the solution and stirred at room temperature for 24 h. The reaction mixture was poured onto ice and treated with 2N HCl and 5% $NaHCO_3$. The organic layers were washed to neutrality with brine, dried over anhydrous Na_2SO_4, filtered and evaporated to dryness. The residue was purified by silica preparative TLC (hexane/EtOAc 2:8) to afford **124** (56 mg, 55%). ^{1}H NMR (400 MHz, $CDCl_3$): δ 2.21 (3H, *s*), 3.10 (3H, *s*), 3.44 (3H, *s*), 3.85 (3H, *s*), 3.88 (3H, *s*), 5.75 (1H, *s*), 6.96 (2H, *d, J* = 8.8), 7.55 (2H, *d, J* = 8.8), 7.89 (1H, *s*), 8.21 (1H, *s*). ^{13}C NMR (100 MHz, $CDCl_3$): δ 24.8 (CH_3), 39.5 (CH_3), 55.6 (CH_3), 55.8 (CH_3), 56.0 (CH_3), 105.9 (CH), 108.9 (CH), 114.0 (2CH), 122.5 (C), 127.1 (C), 130.4 (C), 130.8 (2CH), 144.8 (C), 148.8 (C), 163.5 (C), 168.6 (C). HRMS ($C_{18}H_{22}N_2O_6S + H^+$): calcd 395.1271 ($M + H^+$), found 395.1280.

2.1.41. N-(3,4-dimethoxyphenyl)-4-nitrobenzenesulfonamide (23)

To a solution of 3,4-dimethoxyaniline (2.82 g, 18.41 mmol) in CH_2Cl_2 (50 mL) and pyridine (4 mL), 4-nitrobenzenesulfonyl chloride was slowly added (4.49 g, 20.25 mmol) and stirred at room temperature. After 4 h, the reaction was treated with 2N HCl and 5% $NaHCO_3$, washed with brine to neutrality, dried over anhydrous Na_2SO_4 and concentrated under vacuum to yield 5.43 g (87%) of the sulfonamide **23**. The residue was crystallized in EtOAc to afford the purified compound (4.40 g, 70%). M.p.: 181–183 °C (EtOAc). IR (KBr): 3251, 1532, 1450, 803 cm^{-1}. ^{1}H NMR (400 MHz, $CDCl_3$): δ 3.83 (3H, *s*), 3.84 (3H, *s*), 6.38 (1H, *s*), 6.43 (1H, *dd, J* = 8.4 and 2.4), 6.69 (1H, *d, J* = 8.4), 6.77 (1H, *d, J* = 2.4), 7.87 (2H, *d, J* = 8.8), 8.28 (2H, *d, J* = 8.8). ^{13}C NMR (100 MHz, Acetone-D_6): δ 55.1 (CH_3), 55.2 (CH_3), 107.6 (CH), 111.9 (CH), 114.9 (CH), 124.1 (2CH), 128.6 (2CH), 129.5 (C), 145.2 (C), 147.6 (C), 149.6 (C), 150.2 (C). HRMS ($C_{14}H_{14}N_2O_6S + Na^+$): calcd 361.0465 ($M + Na^+$), found 361.0469.

2.1.42. N-(4,5-dimethoxy-2-nitrophenyl)-4-nitrobenzenesulfonamide (334)

To a solution of **23** (112 mg, 0.33 mmol) in CH_3CN (50 mL) *tert*-butyl nitrite (21.9 μL, 0.16 mmol) was added and stirred at 45 °C. After 24 h, additional 0.16 mmol of *tert*-butyl nitrite was added to the reaction

mixture and it was stirred at 45 °C for another 24 h. Then, the mixture was concentrated, re-dissolved in EtOAc and treated with 5% $NaHCO_3$ solution. The organic layers were washed with brine, dried over Na_2SO_4 and concentrated under vacuum to yield **334** (109 mg, 86%). The residue was purified by crystallization in MeOH to afford 30 mg (24%). M.p.: 169–172 °C (MeOH). ^{1}H NMR (200 MHz, Acetone-D_6): δ 3.88 (3H, *s*), 3.98 (3H, *s*), 7.28 (1H, *s*), 7.57 (1H, *s*), 8.16 (2H, *d, J* = 9), 8.41 (2H, *d, J* = 9). ^{13}C NMR (100 MHz, Acetone-D_6): δ 55.7 (CH_3), 56.1 (CH_3), 105.3 (CH), 107.7 (CH), 124.6 (2CH), 127.4 (C), 128.9 (2CH), 144.4 (C), 146.5 (C), 150.7 (C), 150.7 (C), 155.3 (C). HRMS ($C_{14}H_{13}N_3O_8S + Na^+$): calcd 406.0316 (M + Na^+), found 406.0313.

2.1.43. 4-Amino-N-(3,4-dimethoxyphenyl)benzenesulfonamide (26)

To a solution of **23** (1.96 g, 5.81 mmol) in ethyl acetate (150 mL) and MeOH (5 mL), Pd (C) (10 mg) was added and the reaction was stirred at room temperature under H_2 atmosphere for 48 h. By filtration through Celite® and solvent evaporation, 1.71 g (95%) of **26** was obtained and purified by crystallization in EtOAc (1.39 g, 78%). M.p.: 186–187 °C (EtOAc). IR (KBr): 3449, 3221, 1462, 804 cm^{-1}. ^{1}H NMR (400 MHz, $CDCl_3$): δ 3.73 (3H, *s*), 3.76 (3H, *s*), 4.01 (2H, *s*), 6.02 (1H, *s*), 6.41 (1H, *dd, J* = 8.4 and 2.4), 6.52 (2H, *d, J* = 8.4), 6.61 (1H, *d, J* = 8.4), 6.62 (1H, *d, J* = 2.4), 7.40 (2H, *d, J* = 8.4). ^{13}C NMR (100 MHz, Acetone-D_6): δ 55.0 (CH_3), 55.3 (CH_3), 106.9 (CH), 111.9 (CH), 112.8 (2CH), 113.8 (CH), 126.0 (C), 129.1 (2CH), 131.5 (C), 146.7 (C), 149.4 (C), 152.5 (C). HRMS ($C_{14}H_{16}N_2O_4S + Na^+$): calcd 331.0723 (M + Na^+), found 331.0733.

2.1.44. N-(3,4-dimethoxyphenyl)-4-(dimethylamino)benzenesulfonamide (29)

To a solution of *p*-formaldehyde (1.25 g, 41.11 mmol) in MeOH (40 mL) few drops of acetic acid were added to acid pH, then, 1.27 g of **26** (4.11 mmol) were added and stirred for 30 min. Finally, $NaBH_3CN$ (517 mg, 24.66 mmol) was added and the reaction was heated at reflux for 24 h. The reaction mixture was concentrated, re-dissolved in EtOAc and treated with 2N HCl and 5% $NaHCO_3$ solutions. The organic layers were washed with brine to neutrality, dried over Na_2SO_4, filtered through Celite® and the solvent evaporated in vacuum to afford 1.04 g (75%) of **29**. M.p.: 161–163 °C (EtOAc). IR (KBr): 3467, 3255, 1596, 795 cm^{-1}. ^{1}H NMR (400 MHz, $CDCl_3$): δ 3.01 (6H, *s*), 3.79 (3H, *s*), 3.82 (3H, *s*), 6.09 (1H, *s*), 6.48 (1H, *dd, J* = 8.4 and 2.4), 6.57 (2H, *d, J* = 9.2), 6.68 (1H, *d, J* = 8.4), 6.70 (1H, *d, J* = 2.4), 7.51 (2H, *d, J* = 9.2). ^{13}C NMR (100 MHz, $CDCl_3$): δ 39.9 ($2CH_3$), 55.8 (CH_3), 55.9 (CH_3), 107.2 (CH), 110.6 (2CH), 111.1 (CH), 114.9 (CH), 123.7 (C), 129.1 (2CH), 130.2 (C), 146.7 (C), 148.9 (C), 152.8 (C). HRMS ($C_{16}H_{20}N_2O_4S + H^+$): calcd 337.1217 (M + H^+), found 337.1204.

2.1.45. N-(4,5-dimethoxy-2-nitrophenyl)-4-(dimethylamino) benzenesulfonamide (33)

To sulfonamide **29** (1.17 g, 3.48 mmol) in CH_3CN (50 mL) *tert*-butyl nitrite was added dropwise by two successive additions (460 μL, 3.48 mmol) and the reaction stirred for 24 h at 45 °C. Then, the mixture was concentrated, re-dissolved in EtOAc and treated with 5% $NaHCO_3$ solution. The organic layers were washed with brine, dried over Na_2SO_4 and concentrated under vacuum to produce 1.22 g of crude reaction product from which 949 mg of **33** (71%) was isolated by crystallization in EtOAc. M.p.: 190–195 °C (EtOAc). IR (KBr): 3255, 1593, 1525, 793 cm^{-1}. ^{1}H NMR (400 MHz, $CDCl_3$): δ 3.01 (6H, *s*), 3.86 (3H, *s*), 3.97 (3H, *s*), 6.57 (2H, *d, J* = 9.2), 7.35 (1H, *s*), 7.54 (1H, *s*), 7.63 (2H, *d, J* = 9.2). ^{13}C NMR (100 MHz, $CDCl_3$): δ 40.0 ($2CH_3$), 56.2 (CH_3), 56.7 (CH_3), 102.4 (CH), 107.1 (CH), 110.8 (2CH), 122.9 (C), 129.1 (C), 129.2 (2CH), 131.2 (C), 144.7 (C), 153.2 (C), 155.4 (C). HRMS ($C_{16}H_{19}N_3O_6S + H^+$): calcd 382.1067 (M + H^+), found 382.1067.

2.1.46. N-(2-amino-4,5-dimethoxyphenyl)-4-(dimethylamino) benzenesulfonamide (35)

To nitroderivative **33** (655 mg, 1.72 mmol) in ethyl acetate (100 mL) under H_2 atmosphere, Pd (C) (10 mg) was added and the reaction stirred at room temperature for 48 h. After filtration through Celite® and solvent evaporation 577 mg of **35** (95%) was isolated. M.p.: 153–157 °C (MeOH). IR (KBr): 3403, 1449, 824 cm^{-1}. ^{1}H NMR (400 MHz, $CDCl_3$): δ 3.02 (6H, *s*), 3.49 (3H, *s*), 3.80 (3H, *s*), 5.77 (1H, *s*), 6.00 (1H, *s*), 6.29 (1H, *s*), 6.61 (2H, *d, J* = 9.2), 7.54 (2H, *d, J* = 9.2). ^{13}C NMR (100 MHz, $CDCl_3$): δ 41.2 ($2CH_3$), 56.8 (CH_3), 57.3 (CH_3), 102.1 (CH), 110.0 (CH), 111.8 (2CH), 114.3 (C), 124.9 (C), 130.5 (2CH), 139.9 (C), 142.5 (C), 150.5, (C), 154.1 (C). HRMS ($C_{16}H_{21}N_3O_4S + H^+$): calcd 352.1326 (M + H^+), found 352.1320.

2.1.47. N-(2-amino-4,5-dimethoxyphenyl)-4-(dimethylamino)-N-methylbenzenesulfonamide (118)

To a solution of **35** (155 mg, 0.44 mmol) in CH_3CN (25 mL) 61 mg of crushed KOH (0.88 mmol) and 55 μL of methyl iodide (0.88 mmol) were added and stirred at room temperature for 24 h. Then, the reaction mixture was concentrated, re-dissolved in CH_2Cl_2, washed with brine, dried over anhydrous Na_2SO_4, filtered and concentrated in vacuum to produce 144 mg of crude reaction product from which 105 mg of **118** (65%) was isolated by flash chromatography (hexane/EtOAc 4:6). M.p.: 156–157 °C (MeOH). IR (KBr): 3437, 1462, 812 cm^{-1}. ^{1}H NMR (400 MHz, $CDCl_3$): δ 3.04 (6H, *s*), 3.08 (3H, *s*), 3.47 (3H, *s*), 3.82 (3H, *s*), 5.87 (1H, *s*), 6.33 (1H, *s*), 6.65 (2H, *d, J* = 9.2), 7.52 (2H, *d, J* = 9.2). ^{13}C NMR (100 MHz, $CDCl_3$): δ 38.8 (CH_3), 39.9 ($2CH_3$), 55.7 (CH_3), 56.3 (CH_3), 100.5 (CH), 110.5 (2CH), 111.0 (CH), 118.7 (C), 121.8 (C), 129.9 (2CH), 140.3 (C), 140.8 (C), 149.8 (C), 152.9 (C). HRMS ($C_{17}H_{23}N_3O_4S + H^+$): calcd 366.1482 (M + H^+), found 366.1471.

2.1.48. N-(2-((4-(dimethylamino)-N-methylphenyl)sulfonamido)-4,5-dimethoxyphenyl) formamide (132)

The compound **118** (60 mg, 0.16 mmol) was stirred in a mixture of CH_2Cl_2 (30 mL), pyridine (1 mL) and formic acid (2 mL) at room temperature for 24 h. Then, the reaction mixture was poured onto ice and treated with 2N HCl and 5% $NaHCO_3$, washed to neutrality with brine, dried over anhydrous Na_2SO_4, filtered and solvent evaporated to produce 51 mg of crude reaction product. The residue was purified by silica preparative TLC (hexane/EtOAc 2:8) to afford **132** (31 mg, 50%). ^{1}H NMR (400 MHz, $CDCl_3$): δ 3.05 (6H, *s*), 3.09 (3H, *s*), 3.48 (3H, *s*), 3.91 (3H, *s*), 5.85 (1H, *s*), 6.65 (2H, *d, J* = 9.2), 7.45 (2H, *d, J* = 9.2), 8.00 (1H, *s*), 8.42 (1H, *s*). ^{13}C NMR (100 MHz, $CDCl_3$): δ 39.4 (CH_3), 40.1 ($2CH_3$), 55.8 (CH_3), 56.0 (CH_3), 105.5 (CH), 109.1 (CH), 110.5 (2CH), 120.2 (C), 123.0 (C), 129.9 (2CH), 130.3 (C), 144.9 (C), 148.6 (C), 153.2 (C), 159.1 (CH). HRMS ($C_{18}H_{23}N_3O_5S + Na^+$): calcd 416.1251 (M + Na^+), found 416.1250.

2.1.49. 4-((5,6-Dimethoxy-1H-benzo[d][1,2,3]triazol-1-yl)sulfonyl)-N,N-dimethylaniline (117)

To a solution of **35** (100 mg, 0.28 mmol) in MeOH (20 mL) and H_2O (200 μL) at 0 °C, *tert*-butyl nitrite (33.8 μL, 0.28 mmol) was added and the reaction stirred. After 1 h, acetic acid (20 μL) was added to the reaction mixture and stirred for 24 h to room temperature. Then, the mixture was concentrated, re-dissolved in EtOAc and treated with 5% $NaHCO_3$ solution. The organic layers were washed with brine to neutrality, dried over Na_2SO_4 and concentrated under vacuum. The residue was chromatographed on silica preparative TLC (hexane/EtOAc 1:1) to afford the purified compound **117** (14 mg, 13%). ^{1}H NMR (400 MHz, $CDCl_3$): δ 3.03 (6H, *s*), 3.94 (3H, *s*), 4.04 (3H, *s*), 6.62 (2H, *d, J* = 9.2), 7.34 (1H, *s*), 7.46 (1H, *s*), 7.88 (2H, *d, J* = 9.2). ^{13}C NMR (100 MHz, $CDCl_3$): δ 40.0 ($2CH_3$), 56.2 (CH_3), 56.6 (CH_3), 92.7 (CH), 99.1 (CH), 110.9 (2CH), 120.8 (C), 127.1 (C), 130.0 (2CH), 139.6 (C), 149.2 (C), 152.7 (C), 154.2 (C). HRMS ($C_{16}H_{18}N_4O_4S + H^+$): calcd 363.1122 (M + H^+), found 363.1127.

2.1.50. Methyl 3,5-dinitrobenzoate (80)

3.24 g of 3,5-dinitrobenzoic acid (15.28 mmol) was stirred in a mixture of MeOH (100 mL) and H_2SO_4 (1 mL) for 12 h. Then, anhydrous

Na_2CO_3 was added to the reaction mixture, filtered and concentrated in vacuum. The residue was re-dissolved in EtOAc, washed with water to neutrality, dried over Na_2SO_4 and solvent evaporated. 3.22 g (94%) of the crude reaction product was obtained and used without further purification. ^{1}H NMR (400 MHz, $CDCl_3$): δ 4.06 (3H, *s*), 9.18 (2H, *d, J* = 2.4), 9.24 (1H, *t, J* = 2.4). GC-MS ($C_8H_6N_2O_6$): 226 (M^+).

2.1.51. Methyl 3,5-diaminobenzoate (81)

The compound **80** (3.23 g, 14.27 mmol) was suspended in ethyl acetate (100 mL) and was palladium-catalyzed (Pd (C) 10 mg) reduced under H_2 atmosphere for 72 h. The reaction mixture was filtered through Celite® and the solvent evaporated in vacuum to isolate 2.18 g (92%) of **81**. Crude reaction product was obtained and used without further purification. ^{1}H NMR (400 MHz, $CDCl_3$): δ 3.85 (3H, *s*), 6.18 (1H, *t, J* = 2), 6.77 (2H, *d, J* = 2). GC-MS ($C_8H_{10}N_2O_2$): 166 (M^+).

2.1.52. Methyl 3-amino-5-((4-methoxyphenyl)sulfonamido)benzoate (84A) and methyl 3,5-bis((4-methoxyphenyl)sulfonamido)benzoate (84B)

To a solution of **81** (1.52 g, 9.14 mmol) in CH_2Cl_2 (50 mL) and pyridine (1 mL), was dropwise added 4-methoxybenzenesulfonyl chloride (1.89 g, 9.14 mmol) dissolved in CH_2Cl_2 (20 mL). The mixture was stirred at room temperature for 4 h. Then the reaction was treated with 0.5N HCl washed with brine, dried over anhydrous Na_2SO_4 and concentrated in vacuum. The residue was purified by flash chromatography on silica gel with toluene/EtOAc (7:3) to yield compounds **84A** (375 mg, 12%) and **84B** (957 mg, 41%). **84A:** M.p.: 165–166 °C (CH_2Cl_2/Hexane). IR (KBr): 3468, 3377, 1697, 1497, 1176, 803 cm^{-1}. ^{1}H NMR (400 MHz, $CDCl_3$): δ 3.80 (3H, *s*), 3.84 (3H, *s*), 6.82 (1H, *t, J* = 2), 6.87 (2H, *d, J* = 8.8), 7.01 (1H, *t, J* = 2), 7.09 (1H, *t, J* = 2), 7.71 (2H, *d, J* = 8.8). ^{13}C NMR (100 MHz, CD_3OD): δ 51.1 (CH_3), 54.7 (CH_3), 110.2 (CH), 110.8 (CH), 111.5 (CH), 113.8 (2CH), 128.9 (2CH), 130.9 (C), 131.2 (C), 138.8 (C), 148.9 (C), 163.1 (C), 167.0 (C). HRMS ($C_{15}H_{16}N_2O_5S + H^+$): calcd 337.0853 ($M + H^+$), found 337.0855. **84B:** M.p.: 174–178 °C (CH_2Cl_2/Hexane). IR (KBr): 3270, 1724, 1498, 1150, 802 cm^{-1}. ^{1}H NMR (400 MHz, CD_3OD): δ 3.81 (9H, *s*), 6.94 (4H, *d, J* = 8.8), 7.31 (2H, *d, J* = 2), 7.35 (1H, *t, J* = 2), 7.63 (4H, *d, J* = 8.8). ^{13}C NMR (100 MHz, CD_3OD): δ 51.5 (CH_3), 54.8 ($2CH_3$), 113.8 (4CH), 115.1 (CH), 116.0 (2CH), 129.0 (4CH), 130.6 (2C), 131.5 (C), 139.1 (2C), 163.2 (2C), 165.9 (C). HRMS ($C_{22}H_{22}N_2O_8S_2 + Na^+$): calcd 529.0710 ($M + Na^+$), found 529.0749.

2.1.53. Methyl 3,5-bis((4-methoxy-N-methylphenyl)sulfonamido)benzoate (147)

To a solution of **84B** (132 mg, 0.39 mmol) in acetone (20 mL) K_2CO_3 (542 mg, 3.92 mmol) and $(CH_3)_2SO_4$ (281 μL, 2.94 mmol) were added, heated at reflux and stirred overnight. Then, the reaction mixture was filtered, poured onto ice and extracted with CH_2Cl_2. The organic layers were dried over anhydrous Na_2SO_4, filtered and evaporated to dryness. By crystallization in MeOH compound **147** (73 mg, 51%) was isolated. M.p.: 139–142 °C (MeOH). ^{1}H NMR (400 MHz, $CDCl_3$): δ 3.10 (6H, *s*), 3.84 (6H, *s*), 3.86 (3H, *s*), 6.91 (4H, *d, J* = 8.8), 7.21 (1H, *t, J* = 2), 7.45 (4H, *d, J* = 8.8), 7.66 (2H, *d, J* = 2). ^{13}C NMR (100 MHz, $CDCl_3$): δ 38.1 ($2CH_3$), 52.9 (CH_3), 56.1 ($2CH_3$), 114.7 (4CH), 126.0 (2CH), 127.9 (2C), 129.4 (CH), 130.3 (4CH), 131.7 (C), 142.9 (2C), 163.7 (2C), 165.9 (C). HRMS ($C_{24}H_{26}N_2O_8S_2 + Na^+$): calcd 557.1023 ($M + Na^+$), found 557.1024.

2.1.54. Methyl 3-amino-5-methoxybenzoate (78)

957 mg of 3-amino-5-methoxybenzoic acid (5.73 mmol) was stirred in a mixture of MeOH (50 mL) and H_2SO_4 (1 mL) for 24 h. Then, anhydrous Na_2CO_3 was added to the reaction mixture, filtered and concentrated in vacuum. The residue was re-dissolved in EtOAc, filtered again and evaporated to dryness. 799 mg (77%) of crude reaction product was obtained and used without further purification. ^{1}H NMR (400 MHz, CD_3OD): δ 3.74 (3H, *s*), 3.83 (3H, *s*), 6.48 (1H, *t, J* = 2), 6.84 (1H, *t, J* = 2), 6.95 (1H, *t, J* = 2). ^{13}C NMR (100 MHz, $CDCl_3$): δ 52.1 (CH_3), 55.3 (CH_3), 104.3 (CH), 105.7 (CH), 109.2 (CH), 132.0 (C), 147.6 (C), 160.6 (C), 167.1 (C). GC-MS ($C_9H_{11}NO_3$): 181 (M^+).

2.1.55. Methyl 3-methoxy-5-((4-methoxyphenyl)sulfonamido)benzoate (79)

To a solution of **78** (620 mg, 3.42 mmol) in CH_2Cl_2 (50 mL) and pyridine (2 mL), was slowly added 4-methoxybenzenesulfonyl chloride (707 mg, 3.42 mmol). The mixture was stirred at room temperature for 4 h. Then the reaction was treated with 2N HCl and 5% $NaHCO_3$, washed with brine, dried over anhydrous Na_2SO_4 and the solvent evaporated to obtain 1.15 g (95%) of the sulfonamide **79**. The crude reaction product was purified by crystallization in CH_2Cl_2 (529 mg, 44%). M.p.: 176–177 °C (CH_2Cl_2). IR (KBr): 3258, 1700, 1497, 1152, 802 cm^{-1}. ^{1}H NMR (400 MHz, CD_3OD): δ 3.76 (3H, *s*), 3.81 (3H, *s*), 3.85 (3H, *s*), 6.91 (1H, *t, J* = 2.4), 6.99 (2H, *d, J* = 8.8), 7.20 (1H, *t, J* = 2.4), 7.32 (1H, *t, J* = 2.4), 7.71 (2H, *d, J* = 8.8). ^{13}C NMR (100 MHz, Acetone-D_6): δ 51.6 (CH_3), 54.9 (CH_3), 55.1 (CH_3), 109.6 (CH), 110.2 (CH), 113.1 (CH), 114.2 (2CH), 129.2 (2CH), 131.2 (C), 132.1 (C), 139.6 (C), 160.3 (C), 163.2 (C), 165.6 (C). HRMS ($C_{16}H_{17}NO_6S + H^+$): calcd 352.0849 ($M + H^+$), found 352.0842.

2.1.56. 3-Methoxy-5-((4-methoxy-N-methylphenyl)sulfonamido)benzoic acid (90)

To a solution of **79** (100 mg, 0.28 mmol) in CH_3CN (40 mL) 38 mg of crushed KOH (0.56 mmol) and 36 μL of methyl iodide (0.56 mmol) were added and stirred at room temperature for 24 h. Then, the reaction mixture was concentrated, re-dissolved in CH_2Cl_2, treated with 2N HCl, washed with brine to neutrality, dried over anhydrous Na_2SO_4, filtered and concentrated in vacuum. The residue was purified by silica preparative TLC with CH_2Cl_2 (98:2) yielding compound **90** (69 mg, 66%). M.p.: 186–187 °C (CH_2Cl_2). IR (KBr): 3000, 1689, 1502, 806 cm^{-1}. ^{1}H NMR (400 MHz, CD_3OD): δ 3.16 (3H, *s*), 3.79 (3H, *s*), 3.86 (3H, *s*), 6.94 (1H, *t, J* = 2.4), 7.03 (2H, *d, J* = 8.8), 7.26 (1H, *t, J* = 2.4), 7.46 (1H, *t, J* = 2.4), 7.47 (2H, *d, J* = 8.8). ^{13}C NMR (100 MHz, $CDCl_3$): δ 37.8 (CH_3), 55.6 (CH_3), 55.7 (CH_3), 113.8 (CH), 114.0 (2CH), 118.7 (CH), 119.3 (CH), 127.7 (C), 129.9 (2CH), 130.9 (C), 143.1 (C), 159.7 (C), 163.2 (C), 170.6 (C). HRMS ($C_{16}H_{17}NO_6S + H^+$): calcd 352.0849 ($M + H^+$), found 352.0848.

2.2. Determination of aqueous solubility

The aqueous solubility of the sulfonamides was determined in a Helios Alfa Spectrophotometer using an approach based on the saturation shake-flask method. 1–2 mg of each tested compound was suspended in 300 μL pH 7.0 buffer and stirred for 72 h at room temperature. The resulting mixture was filtered over a 45 μm filter to discard the insoluble residues. Then, a scan between 270 and 400 nm was performed and the three maximum wavelengths were selected for each compound. Calibration curves were performed at these wavelengths and the concentration in the supernatant was measured by UV absorbance.

2.3. Cells and culture conditions

The *L. infantum* strain used in this study was MCAN/ES/MON1/Z001. The myeloid human cell line used, originally obtained from a patient with histiocytic leukemia was U937 (ATCC® CRL1593.2). The human tumor cell lines were HT-29, HeLa, and MCF7, obtained from a patient with colon, cervical, and breast cancer respectively.

Leishmania promastigotes were cultured at 27 °C in RPMI 1640 supplemented with L-glutamine (Lonza-Cambrex, Karlskoga, Sweden), 10% heat-inactivated fetal bovine serum (HIFBS) (Lonza-Cambrex), and 100 μg/mL streptomycin-100 IU/mL penicillin (Lonza-Cambrex) in 25 mL culture flasks. Logarithmic and late stationary promastigotes were obtained after incubation for 3–4 and 6–7 days respectively. The starting inoculum was $4{\cdot}10^6$ parasites/mL.

Leishmania axenic amastigotes were obtained from late stationary

promastigotes. After harvesting promastigotes at 250 g for 10 min, they were centrifuged in Percoll® (Sigma) gradient to select the living population. Then, promastigotes were seeded at $4{\cdot}10^6$ parasites/mL in M199 medium (Invitrogen, Leiden, The Netherlands) supplemented with 10% HIFBS, 1 g/L β-alanine, 100 mg/L L-asparagine, 200 mg/L sucrose, 200 mg/L D-fructose, 50 mg/L sodium pyruvate, 320 mg/L malic acid, 40 mg/L fumaric acid, 70 mg/L succinic acid, 200 mg/L α-ketoglutaric acid, 300 mg/L citric acid, 1.1 g/L sodium bicarbonate, 5 g/L morpholineethanesulfonic acid (MES), 0.4 mg/L hemin, 10 mg/L gentamicin and 100 μg/mL streptomycin-100 IU/mL penicillin; pH 5.4, at 37 °C in a 95% humidity, 5% CO_2 atmosphere. After 24h of incubation, all parasites had a round morphology without an emerging flagellum.

U937 (human lung histiocytic lymphoma) and HT-29 (human colon carcinoma) cells were cultured at 37 °C in complete RPMI 1640 medium (see above) in a 95% humidity, 5% CO_2 atmosphere. HeLa (human cervical carcinoma) and MCF7 (human breast carcinoma) cell lines were cultured in DMEM medium containing 10% (v/v) HIFBS, 2 mM L-glutamine and 100 μg/mL streptomycin-100 IU/mL penicillin at 37 °C in 95% humidity, 5% CO_2 atmosphere.

2.4. Cytotoxicity assays

The effect of the different compounds on the proliferation of human tumor cell lines was determined by using the XTT (sodium 3,39-[1(phenylaminocarbonyl)-3,4-tetrazolium]-bis(4-methoxy-6-nitro)benzene sulfonic acid hydrate) cell proliferation kit (Roche Molecular Biochemicals, Mannheim, Germany) as previously described (Scudiero et al., 1988). Briefly, a freshly prepared mixture solution of XTT labeling reagent and PMS (N-methyl-dibenzopyrazine methyl sulfate) electron coupling reagent was added to cells and were incubated during the corresponding time according to each cell line (6 h for U937 and HT-29 and 4 h for HeLa and MCF7 cells), in a humidified atmosphere (37 °C, 5% CO_2), and the absorbance of the formazan product generated was measured at a test wavelength of 450 nm. A positive control is formed by cells without compounds at 72 h and a negative control is formed by cells without compounds at 0 h of incubation. Measurements were performed in triplicate, and each experiment was repeated three times.

Cell viability was evaluated seeding 100 μL of cells in exponential growth phase with appropriate cell line concentration ($1{\cdot}10^5$ U937 cells/mL, $3{\cdot}10^4$ HT-29 cells/mL, $1.5{\cdot}10^4$ HeLa cells/mL and $1.5{\cdot}10^4$ MCF7 cells/mL) in complete RPMI 1640 or DMEM medium in 96-well plates at 37 °C and 5% CO_2. The tested sulfonamides were added at 10 μM after 24 h of incubation, to attached U937 cells and 1 μM to HT-29, HeLa, and MCF7 cells. The effect on proliferation was evaluated 72 h post-treatment. The compounds were dissolved in dimethyl sulfoxide (DMSO) and the final solvent concentrations never exceeded 0.5% (v/v).

2.5. Leishmanicidal assays

The leishmanial growth inhibition assays in promastigotes and axenic amastigotes were performed by using the XTT method described above.

2.5.1. In vitro promastigote assay

The *in vitro* promastigote susceptibility assay was performed with logarithmic and late stationary promastigotes including two independent replicates. 100 μL of promastigotes in complete RPMI 1640 medium were seeded at $4{\cdot}10^6$ parasites/mL in 96-well plates at 27 °C, in the absence and the presence of 10 μM concentration of the corresponding sulfonamides. The compounds were dissolved in DMSO. The final solvent concentrations never exceeded 0.5% (v/v). After 24 h incubation, each plate-well was examined by light microscopy to detect changes in parasite morphology or motility. 72 h after treatment, 50 μL of XTT solution were added to each well, and the cells were incubated for 7 h at 27 °C. Thereafter, absorbance was measured at 450 nm with a MicroPlate Reader 680 spectrophotometer and MicroPlate Manager 5.2.1. software (BioRad). Measurements were done in triplicate, and each experiment was repeated three times.

2.5.2. Axenic amastigote assay

Axenic amastigote viability assays were performed following a similar method. Promastigotes were differentiated into axenic amastigotes as previously described. 100 μL of late stationary promastigotes were seeded at $4{\cdot}10^6$ parasites/mL in complete M199 medium in 96-well plates at 37 °C. After 24 h incubation sulfonamides at different concentrations (a first screening using 10 μM and then 15, 10, 9, 7, 6, 4, 2, and 1 μM of active compounds) were added to axenic amastigotes. Then, the XTT solution was added 48 h post-treatment and incubated for 7 h at 37 °C. The efficacy of each compound was estimated by calculating the IC_{50} (half maximal inhibitory concentration). Measurements were done in triplicate, and each experiment was repeated three times.

2.5.3. In vitro macrophage infection and intracellular amastigote assay

The *in vitro* infection of the human U937 myeloid cell line with *L. infantum* promastigotes was carried out to evaluate the antileishmanial activity of new sulfonamides. U937 cells were centrifuged at 250 g for 10 min. Then, 400 μL of cells in complete RPMI 1640 medium were seeded at $3.75{\cdot}10^5$ cells/mL in 8-well chambers slides (LabTek, New York, NY) at 37 °C and were differentiated by stimulation with 20 ng/ml phorbol 12-myristate 13-acetate (PMA) (Sigma, Saint Louis, MO) for 72 h. The cultures were rinsed three times with complete RPMI medium to remove nondifferentiated unattached cells. Then, cells were infected with stationary *L. infantum* promastigotes at 37 °C at a 5:1 promastigote:macrophage ratio in 400 μL complete RPMI medium in an atmosphere of 5% CO_2 for 2 h. Noninternalized promastigotes were removed by 3–4 successive washes with complete RPMI medium. Then, infected macrophages were incubated in complete medium with sulfonamides at different concentrations (first screening using 20 μM, then 20, 15, 10, 7, and 5 μM for active compounds) for 48 h. The compounds were dissolved in DMSO and the final solvent concentrations never exceeded 0.5% (v/v). Finally, fixation and staining were performed. For this purpose, the wells were first washed three times with fresh complete medium. Then, the cells were treated with hypotonic solution (complete medium:water 9:11) for 5 min and were fixed with 150 μL ethanol:acetic acid 3:1 for 10 min (step repeated three times). The preparations were allowed to air dry and the wells were removed from the slide. Modified Giemsa staining was carried out with Diff-Quick® Stain Solution I and II (Dade Behring, Marburg, Germany). The preparations were washed with distilled water, air-dried, and mounted with Entellan® Neu (Merck, Darmstadt, Germany). The number of amastigotes per infected cell was estimated by counting 100 cells per biological replicate randomly. The experiment was performed in triplicate and the statistical analysis was based on Student's paired *t*-test.

2.6. Docking studies

The sequences of α and β tubulins from *Leishmania* with sizes larger than 400 amino acids were retrieved from UniProt (Bateman, 2019). Sequences were aligned with each other and with the sheep tubulin sequence of the pdbID 3HKC X-ray structure from the Protein Data Bank (Berman et al., 2003) using ClustalX (Larkin et al., 2007). The amino acids forming the colchicine domain were defined and selected as those closer than 6 Å to the ligands in the colchicine site of the tubulin-colchicine site ligand complex X-ray structures published in PDB. The comparison of 20 *Leishmania* sequences with the sheep sequence indicated changes at 11 amino acid residues with sidechains contacting colchicine site ligands. Eight of them were conserved in the *Leishmania* sequences and all three that changed (i.e. N167β, K254β, and I347β) could be represented by just four sequence combinations used for building the homology models. The sheep 3HKC X-ray structure was used as a template for the generation of the homology models for two

reasons: i) the ABT-751 ligand is one of the very few ligands binding to the 3 zones (1–3) of the colchicine site; and ii) said ligand has an *N*-aryl-methoxybenzenesulfonamide structure in common to the compounds in our library. Hence, it provides the most favorable starting point for the docking studies, as confirmed by successful cross-dockings of other ligands with known X-ray structures binding at zones 1, 2, or 3, like combretastatin A-4 (sites 1 and 2) or nocodazole (sites 2 and 3). 5 homology models were generated with Modeller 9.15 (Šali and Blundell, 1993) for each sequence combination, for a total of 20 homology models for the *Leishmania* proteins. The models were curated manually to avoid the colchicine binding site collapse previous to the docking experiments. Docking studies of the ligands in the mammalian proteins and the *Leishmania* homology models were carried out as described (Álvarez et al., 2013). Additionally, representative ligands binding at zones 1, 2, and/or 3 of the colchicine site were docked and compared with their X-ray complex structures to validate the selection of 3HKC as a template. Docking runs were performed with PLANTS with default settings (Korb et al., 2009) and generated 10 runs per ligand. AutoDock 4.2 (Forli et al., 2016) runs applied the Lamarckian genetic algorithm (LGA) 100–300 times for a maximum of 2.5×10^6 energy evaluations, 150 individuals, and 27000 generations maximum. The poses were automatically assigned to zones 1–3, and the results tabulated using in-house KNIME pipelines (Berthold et al., 2007). Z-scores were generated from the programs' scores. The results were analyzed with Chimera (Pettersen et al., 2004), Marvin ("Marvin 17.8 ChemAxon," 2017), OpenEye ("OpenEye Scientific Software, Inc, Santa Fe," 2019), and JADOPPT (Garcia-Perez et al., 2017).

3. Results and discussion

3.1. Chemical library design

The search for new antiparasitic drugs, including antileishmanial compounds has followed two distinct approaches: i) the blind screening of large compound libraries (HTS) that impair parasite viability, the so-called phenotypic assays; or ii) or target-based screenings where ligands acting on a particular target of interest are sought (Zulfiqar et al., 2017). The first approach has the advantage of guaranteeing effects on the whole organism and therefore fulfilling pharmacokinetic and pharmacodynamic requirements and finds drugs active against unforeseen targets. However, it has the disadvantage of requiringing challenging target deconvolution in the following drug development process. Target-based screens, on the other hand, have the advantage of facilitating later stages of drug development, although the compounds do not always have

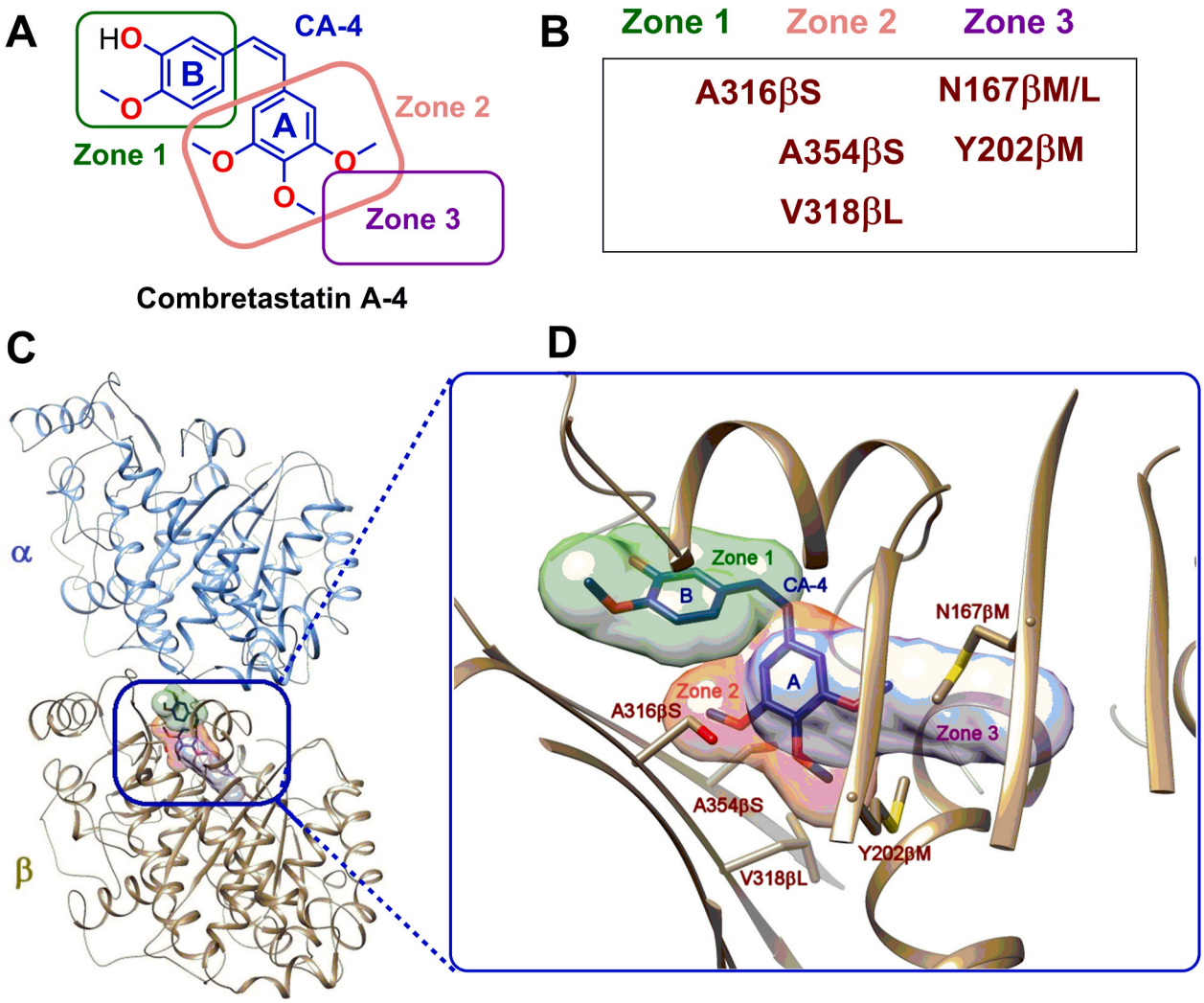

Fig. 1. The tubulin colchicine site and differences between mammals and *Leishmanias*. (**A**) Chemical structure of combretastatin A-4 with the interaction zones indicated by colored rectangles. (**B**) Amino acid substitutions in trypanosomatids compared to mammals. (**C**) Ribbon model of the tubulin dimer with combretastatin A-4 bound in the colchicine site, indicated by a blue rectangle. (**D**) Detail of the colchicine-binding site with the three binding zones indicated as colored volumes and with the amino acids of the *Leishmania* sequences which vary from humans shown. (For interpretation of the references to color in this figure legend, the reader is referred to the Web version of this article.)

adequate pharmacokinetic properties, or the target turns out to be non-essential and lacks activity in the whole organism. Herein, an intermediate approach has been adopted by designing a focused library against the well validated target tubulin and assaying the compounds in a phenotypic screen against several stages of the parasite life cycle. As a result, both pharmacokinetic and pharmacodynamic issues were simultaneously assessed to achieve a basis of the mechanism of action.

Trypanosomatid microtubules present up to 11 different amino acid substitutions in the colchicine-binding site relative to mammalian orthologs (Luis et al., 2013). To determine sequence differences from humans to *Leishmania* potentially affecting the binding of colchicine site ligands, the colchicine site was defined as any set of tubulin amino acid residues whose sidechain is less than 6 Å away from the ligand complexed at said site. More than 50 colchicine site ligands complexed with tubulin retrieved from Protein Data Bank (PDB) (Berman et al., 2003; Vicente-Blázquez et al., 2019) were considered. The study determined sequence differences between the human and the *Leishmania* ortholog affecting ligand binding to the colchicine site. Clustal X (Larkin et al., 2007) alignment of the X-ray structure sequences with the *Leishmania* sequences retrieved from UniProt (Bateman, 2019) and comparison of the amino acids assigned to the colchicine site allowed for identifying mutated residues (Fig. 1). The colchicine domain in tubulin has been subdivided into three sub-pockets (1-3). Zzones 1–3 bind several moieties of typical colchicine site ligands, such as combretastatin A-4 (Fig. 1) and nocodazole. Zone 1 (Massarotti et al., 2012) is the pocket for combretastatin A-4 ring B. Sequence conservation between leishmanial and human tubulin is high in this pocket. The sole exception is the A316βS replacement, located at the inner edge of the V-shaped A and B rings of combretastatin A-4. It makes the gap smaller but more polar due to the presence of the serine side chain hydroxyl group. Therefore, small modifications were envisaged for B-rings, except for the introduction of non-bulky hydrogen bond acceptors and donors such as small amine or formamide groups. *Leishmania* tubulin sequences show an A250βS change compared to the sheep ortholog in the pocket accommodating the bridge connecting zones 1 and 2, located in a flexible loop at the interface between tubulin subunits. The hydroxyl group in this region suggested the introduction of a sulfonamide to bridge the A and B rings. *Leishmania* tubulin sequences contain the substitutions A316βS, A354βS, C241βT, and V318βL in zone 2. These changes configure a smaller and more polar pocket compared to the mammalian protein due to three additional hydroxyl groups. This suggested the possibility of removing some of the methoxyl groups from the classical trimetoxyphenyl A ring of combretastatin A-4 and the introduction of additional hydrogen bonding groups. These modifications may also probably reduce activity against human tubulin, thus conferring selectivity. Finally, zone 3 contains the N167βI and the Y202βM substitutions. This zone would become smaller and less polar, thus leaving the negatively charged D200β in a very hydrophobic environment. However, mutations in zone 3 have been described in parasites resistant to benzimidazoles. Hence, this zone was not pursued (Furtado et al., 2016).

Considering these sequence differences between the tubulin of Leishmania and the mammalian hosts at the colchicine site, a focused library of 350 compounds was designed by a combination of several substitutions on a diarylsulfonamide scaffold and later synthesized. The

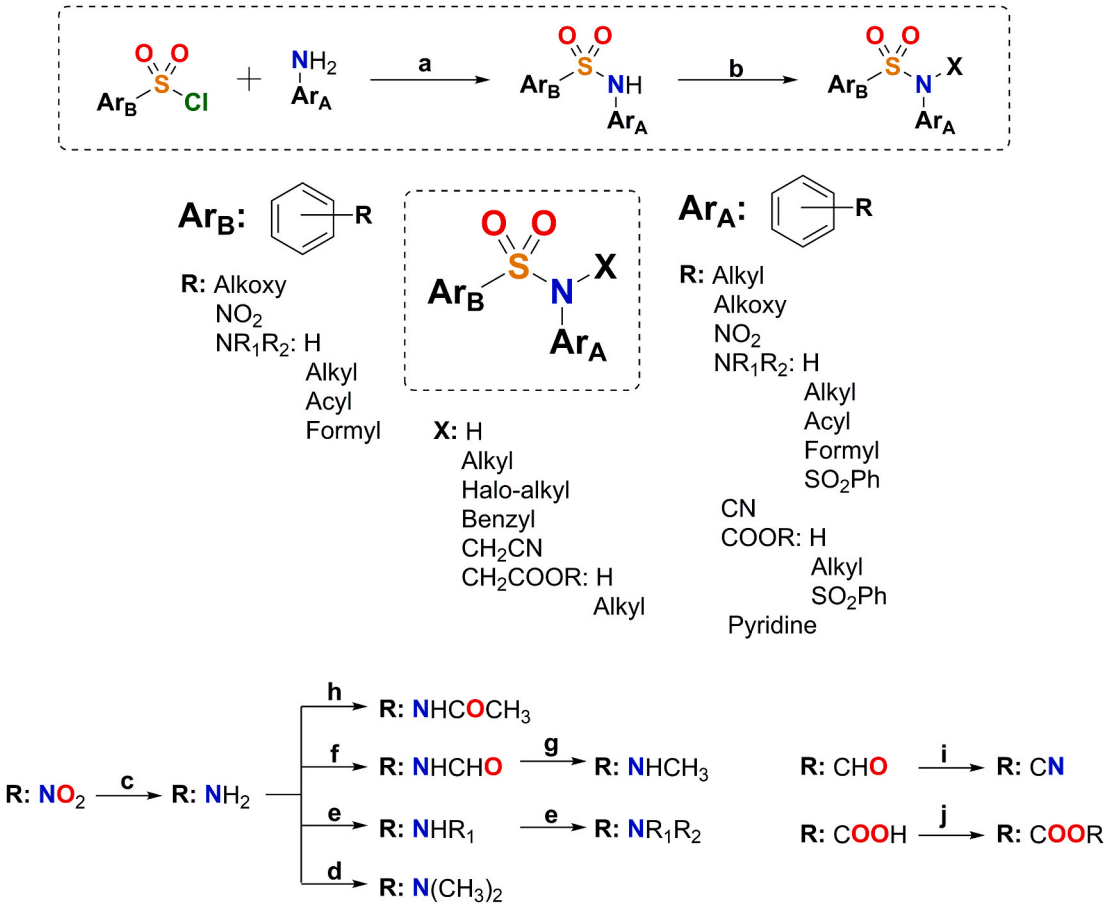

Fig. 2. General structure of diarylsulfonamide library. General chemical synthetic route for the chemical library of 350 diarylsulfonamides: (a) Pyridine, CH_2Cl_2, rt, 1 h. (b) X-Halogen, K_2CO_3, DMF, rt, 12 h. (**B**) Some of the most frequent modifications carried out in aromatic ring B (Ar_B) and/or aromatic ring A (Ar_A) substituents. Structural variations in the library and main functional group modifications: (c) H_2, Pd/C, EtOAc, rt, 48 h. (d) *p*-formaldehyde, $NaBH_3CN$, AcOH, MeOH, reflux, 2 h. (e) R-Halogen, CH_2Cl_2, rt, 1–12 h. (f) Formic acid, CH_2Cl_2, rt, 24 h. (g) Trichloroacetic acid, $NaBH_4$, THF, rt, 12 h. (h) Acetic anhydride, CH_2Cl_2, rt, 30 min. (i) 1) $NH_2OH{\cdot}HCl$, pyridine, MeOH, reflux 24 h. 2) Acetic anhydride, pyridine, reflux, 48 h. (j) R–OH, H_2SO_4, rt, 3 h.

substitutions were selected with two purposes: i) fitting the structural requirements of the parasite tubulins; and ii) avoiding binding to the mammalian counterparts. These substitutions are schematically shown in Fig. 2, altogether with the general synthetic route applied to build the library. According to the observed sequence differences for zone 2, the trimethoxyphenyl ring of mammalian anti-tubulin ligands has been replaced with dimethoxyphenyl rings bearing the methoxy groups in different positions, methoxypyridines, carboxyanilines, and others. All the compounds were isolated, purified, and chemically characterized. Herein, the synthetic details described in the Methods section and below for the active compounds are described. The synthesized compounds are readily available, chemically stable, and possess drug-like properties (Supp Mat Table 1) (Daina et al., 2017), in good agreement with the requests for new antileishmanial therapies.

3.2. Chemical synthesis

The construction of the diarylsulfonamide scaffolds was performed through the reaction between sulfonyl chlorides and primary amines (Fig. 2). The reactions occurred in good yields (85–98%) and could be easily prepared in large amounts for later modifications. Non-commercial amines required for the synthesis of the sulfonamide bridge were obtained by the nitration of the correspondent aromatic rings, and subsequent palladium-catalyzed reduction. When further substituent modifications on the ring were required, they were carried out before the introduction of the amine groups. Occasionally, for aryls with two amino groups or with an amino group and a carboxylic acid group simultaneously, products with three aromatic rings were also obtained (e.g. **63B, 147**). Diarylsulfonamides with amine or amine derivative substituents were prepared after sulfonamide assembly from nitro groups and later functional group modification. Substitutions on the sulfonamide nitrogen were introduced by alkylation reactions. Bromination reactions were performed when necessary. Detailed chemical synthesis of compounds that showed antileishmanial activity can be found in materials and methods and the structures of all the synthesized compounds are available from the authors upon request.

3.3. Solubility and chemical stability

The low stability and low aqueous solubility of 1 μg/mL (Vandermeulen et al., 2006) are the main pharmacokinetic drawbacks of Amphotericin B. This drug is generally administered in sodium deoxycholate or liposomal formulations and needs special storing and transport conditions. This increases the cost and treatment difficulty. All the prepared compounds remained stable for more than 48 h in solution at room temperature, as determined by ^{1}H-NMR. Most of them are crystalline solids that remain unaltered for weeks at room temperature. The solubility of representative active compounds of the series in phosphate buffer at pH 7.0 was determined as follows: i) shaking in pH 7.0 phosphate buffer for 72 h; ii) microfiltration; and iii) identification and quantification by UV absorbance at three different wavelengths. Compounds **26**, **35**, and **63B** showed thermodynamic solubilities of 55 μg/mL, 118 μg/mL; and, 1889 μg/mL, respectively. These are moderate to good aqueous solubilities, which is an important parameter for the oral administration of drugs.

3.4. Cytotoxicity in human cells

The effect of the synthesized sulfonamides on the cellular proliferation of four human tumor cell lines: U937 (human lung histiocytic lymphoma), HT-29 (human colon carcinoma), HeLa (human cervical carcinoma), and MCF7 (human breast adenocarcinoma), was studied as a surrogate of human toxicity and to select the least cytotoxic compounds against human cells for the *in vitro* leishmanicidal assays (Table 1). The compounds were tested at concentrations of 10 μM for the U937 and 1 μM for HT-29, HeLa, and MCF7 cell lines. Most compounds did not show antiproliferative effects at the concentrations studied, which might be due to the structural modifications introduced to reduce binding to mammalian tubulin. The more cytotoxic compounds were those with bulky substituents on the sulfonamide nitrogen, such as a benzyl group in the 3,5-dimethoxyaniline series (e.g. compounds **332, 326B,** and **275**) and/or a bromine atom on the 2,5-dimethoxyaniline series (for example, **204, 332** and **326B**) (Table 1, Fig. 3). After evaluating antileishmanial activity (see below), the IC_{50} values of antiproliferative activity against the human cancer cell line HeLa were determined, and selectivity indexes were calculated (Supplemental Table S1). The best selectivity indexes correspond to compound **276B**, with values of 11.5 for axenic amastigotes and 3.45 for intracellular amastigotes.

3.5. Activity in leishmania promastigotes

The 350 sulfonamides under study were tested for their antiprotozoal activity against logarithmic and late stationary cultured *L. infantum* promastigotes (MCAN/ES/MON1/Z001). Cell proliferation was assessed 72 h after drug treatment at 10 μM using the XTT method and compared with untreated cells taken as 100% of proliferation. None of the compounds was active against this parasite stage at the tested concentration. However, this is not a requirement for treatment. Promastigotes are not the mammalian stage, unlike intracellular amastigotes. Noticeable differences in gene expression profiles have been found between them (Almeida et al., 2004; Leifso et al., 2007). Hence, active compounds should target amastigotes.

3.6. Activity in axenic amastigotes

Since *Leishmania* spp amastigotes are responsible for all clinical manifestations in humans and studying intracellular amastigotes is challenging, the compounds were first tested against axennic amastigotes. This allowed for selecting the best candidates for subsequent assays with intracellular amastigotes. *L. infantum* axenic amastigotes were differentiated from late stationary promastigotes by temperature, pH, and culture medium shift. All compounds were tested using the XTT method after 48 h of treatment initially at 10 μM. Those significantly active were selected for IC_{50} calculation. Measurements were done in triplicate, and each experiment was repeated three times. Eight compounds out of 350 (2.3%) showed potencies better than 10 μM against axenic amastigotes (Table 1). Three of them (**129, 204,** and **332**) behaved like or better than miltefosine. Compound **129** was the most potent of the series with sub-micromolar potency and did not show cytotoxicity against the human cancer cell lines. Five additional compounds had satisfactory IC_{50} values between 5 and 12 μM (**326B, 275, 279, 334** and **276B**) (Table 1). Series including several active compounds are phenyl sulfonamides of 2,5-dimethoxy- (**129, 204** and **332**) and 3,5-dimethoxy- (**275**, **326B**) anilines. The first series includes all three most potent compounds. The introduction of a bromo substituent in this series renders the compounds (**204**, **326B,** and **332**) cytotoxic. Nevertheless, the most potent compound of the series (**129**) is not cytotoxic at the tested concentrations. The allowed substituents on the phenylsulfonamide include the methoxy groups and both monomethyl and dimethylamines. Additional substituents on the ring are also tolerated. These results indicate a more permissive binding pocket of the target for these moieties. Interestingly, the larger triaryl compound **276B** is also active against axenic amastigotes but not cytotoxic. These results show that small structural changes can result in selective activity against axenic amastigotes without affecting the host cells. These non-cytotoxic compounds are considered ideal candidates for further development as leishmanicidal drugs.

3.7. Activity against intracellular amastigotes

Intracellular amastigotes are the clinically relevant infective stage of

Table 1
Leishmanicidal and cytotoxic activities of sulfonamides that showed antileishmanial activity in any of the parasite stages.

Compound	*Leishmania infantum*			U937 10 μM	HT-29 1 μM	HeLa 1 μM	MC7 1 μM
	Promastigotes	Axenic amastigotes	Intracellular amastigotes				
	10 μM	IC_{50} (μM)	20 μM				
129	NA	0.93	A	NC	NC	NC	NC
138	NA	NA	A	NC	NC	NC	NC
204	NA	2.2	ND	C	C	C	C
183	NA	NA	A	NC	NC	NC	NC
332	NA	4.3	ND	C	C	C	C
326B	NA	8.2	ND	C	C	C	C
275	NA	8.1	ND	C	NC	NC	NC
242	NA	NA	A	NC	NC	NC	NC
320	NA	NA	A	NC	NC	NC	NC
316	NA	NA	A	NC	NC	NC	NC
279	NA	12	NA	NC	NC	NC	NC
334	NA	5.75	NA	NC	NC	NC	NC
124	NA	NA	A	NC	NC	NC	NC
132	NA	NA	A	NC	NC	NC	NC
117	NA	NA	A	NC	NC	NC	NC
35	NA	NA	A	NC	NC	NC	NC
26	NA	NA	A	NC	NC	NC	NC
84	NA	NA	A	NC	NC	NC	NC
90	NA	NA	A	NC	NC	NC	NC
147	NA	NA	A	NC	NC	NC	NC
63B	NA	NA	A	NC	NC	NC	NC
276B	NA	6.7	A	NC	NC	NC	NC
Miltefosine	A	4.4	A	NC	ND	ND	ND

Leishmanicidal activities of sulfonamides on *L. infantum* promastigotes and axenic amastigotes at 10 μM and IC_{50} calculation; on intracellular amastigotes at 20 μM and cytotoxicity on human tumor cell lines U937 at 10 μM and HT-29, HeLa and MCF7 at 1 μM. NA, Inactive at tested concentration. A, Active at tested concentration. NC, Not Cytotoxic at tested concentration. C, Cytotoxic at tested concentration. ND, Undetermined. Assays are described in Materials and Methods.

Leishmania spp. in mammals. They frequently show different drug sensitivities from promastigotes or axenic amastigotes (Zulfiqar et al., 2017). The intracellular leishmanicidal activity was assayed in amastigote-infected U937 cells. Infection was performed by incubation with stationary *L. infantum* promastigotes. Then, infected macrophages were incubated with treatment compounds for 48 h. After fixation and staining of the samples, activity was determined by randomly counting the number of amastigotes per infected cell. Activity against intracellular amastigotes at 20 μM was evaluated for all compounds in the library not inducing cytotoxicity in U937 cells used for infection at 10 μM (157 compounds). 16 compounds showed activity against intracellular amastigotes (Table 1), 10% of the tested compounds and 5% of the total: very high success rates. More compounds were active against intracellular than axenic amastigotes. Promastigotes are usually more sensitive than amastigotes to most compounds tested elsewhere (De Muylder et al., 2011). The diarylsulfonamide inhibitors detailed above are an exception.

Among the eight active compounds against axenic amastigotes (Table 1), four are cytotoxic to U937 cells and two are inactive against intracellular amastigotes (i.e. **279** and **334**). Just two, i.e. **129** and **276B** (Fig. 4), are active against both amastigote forms and not cytotoxic. Box Plot data analysis of the number of amastigotes per cell (Fig. 4A) showed that the infection progress is inversely proportional to the ligand concentration compared with untreated control cells. 75% of the analyzed cells host 0–1 amastigote per cell when treated with active compounds (Fig. 4B). The same percentage of untreated cells accommodate 0–4 amastigotes per cell. The maximum reached 6–9 amastigotes per cell under different treatments and 15 in the untreated control. Hence, late stationary *L. infantum* promastigotes infected the U937 macrophages and subsequently differentiated into intracellular amastigotes, divided into the host cell, and infected other cells in the untreated control, whereas the evidence shown in Table 1 and Figs. 4 and 5 suggests that at least one of these steps may have been partially blocked in treated cells by a few compounds. Compound **129** leads to the most remarkable decrease in the infection measured in terms of the percentage of infected cells and the number of amastigotes per infected cell. Sulfonamides **279** and **334** with activity against axenic amastigotes did not show activity against intracellular amastigotes. The reason could be differences in cellular uptake or to the reported biochemical differences between both amastigote forms (Alcolea et al, 2010, 2014; Rochette et al., 2009).

Interestingly, a high proportion of compounds (14 out of 16) showed activity against intracellular amastigotes but not against axenic amastigotes (Table 1 and Fig. 6). This discrepancy could be due to the different threshold applied for considering positives, but the number of examples suggests a more probable host-cell-dependent mechanism of action (De Muylder et al., 2011). These results and the subtle differences between mammalian and parasitic tubulins suggest the possibility of an action on the host tubulin at sub-cytotoxic concentrations, which has been previously shown in the treatment of eukaryotic cells with tubulin inhibitors, contributing to the antileishmanial activity. The well-known capability of tubulins of different origins, specifically mammalian and leishmanial, to co-assemble and exchange dimer subunits would support the possibility of a tubulin-mix based mechanism (Montecinos-Franjola et al., 2019). Aside from compounds only active against intracellular amastigotes (**138** and **183** from the 2,5-dimethoxyphenyl, **242** from the 3,5-dimethoxyphenyl, and **316** and **320** from the 6-methoxy-3-pyridyl series) (Fig. 3 and Table 1), new structural types of phenyl sulfonamides are also active against intracellular amastigotes: i) 3,4-dimethoxyanilines (**26**, **35**, **117**, **124**, **132**, and **334**, the latter also active against axenic amastigotes); ii) 3-carboxy-5-aminoanilines (**84A**, **90**, and **147**); and the triaryl **63B**.

3.8. Docking studies

To obtain insights into tubulin-binding of the active compounds, we have performed flexible docking studies with mammalian and leishmanial tubulins. Protein flexibility was accounted for by using several structures with different binding-site configurations. For the mammalian proteins, we used 50 X-Ray crystal structures of complexes with different ligands bound to the colchicine domain available in PDB and five more representative models from a molecular dynamics simulation, as described (Álvarez et al., 2013). For the leishmanial tubulin, 5

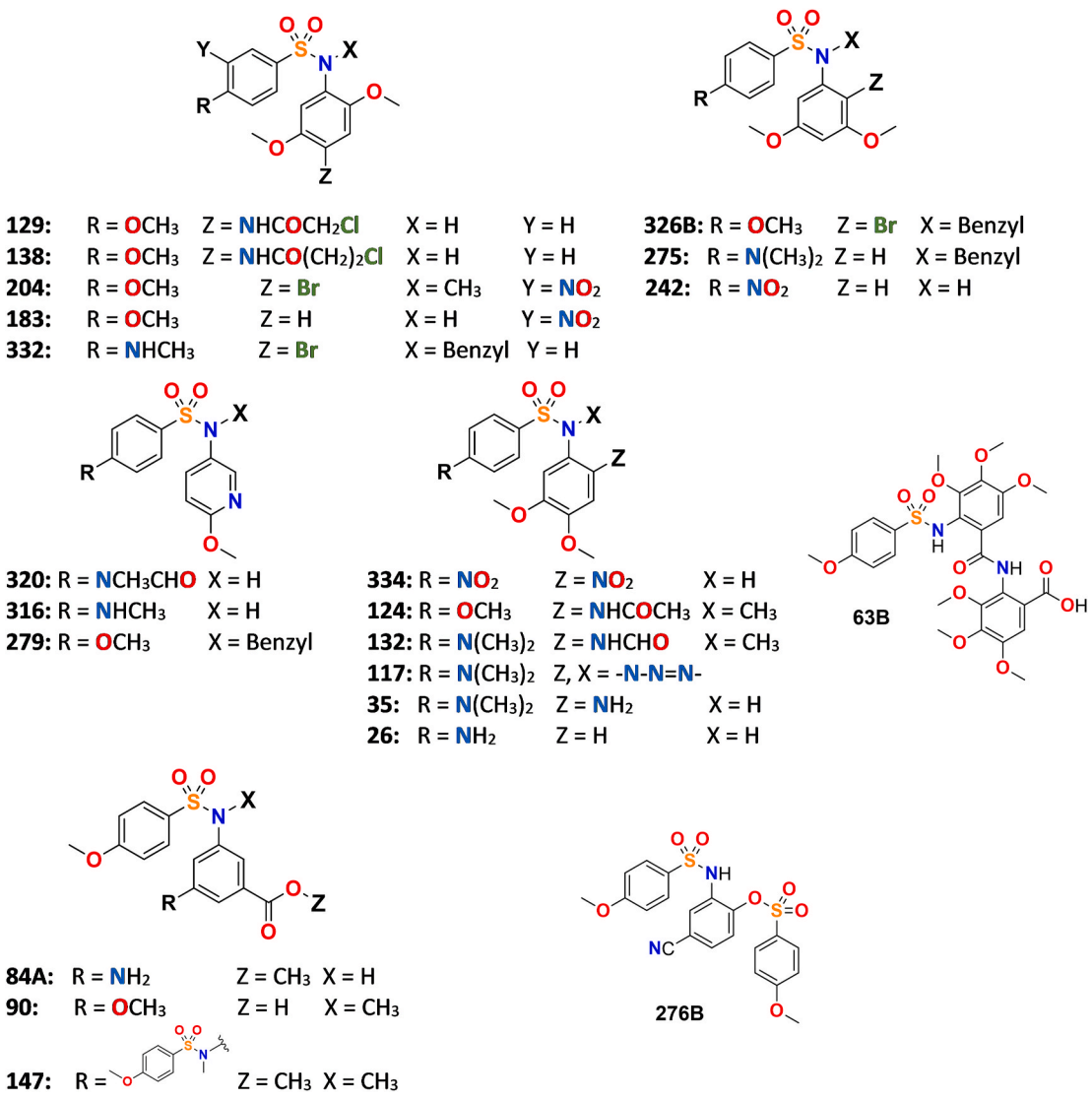

Fig. 3. Structures of the tested sulfonamides that showed leishmanicidal activity.

homology models were generated with Modeler (Šali and Blundell, 1993) for each unique combination of amino acids in the colchicine site present in the leishmanial sequences retrieved from UniProt. As a result, 20 models of leishmanial tubulin were used for the docking studies. These studies were performed with two frequently used docking programs that use very different scoring functions. For each ligand, several thousand poses were generated bound to each of the protein sets. The poses were automatically assigned to the occupied zones (A-D) of the binding domain. Those showing the best consensus scores returned by both programs were selected as the binding poses (Fig. 7) (Supp Mat Table 2).

Most ligands bind in similar ways to the mammalian and the leishmanial protein, occupying sites A and B (Fig. 7). Even the apparently large ligand **276B** for a colchicine-site ligand binds similarly to ABT-751 (Supplemental Fig SF1. The phenyl rings with the larger substituents are always located in zone 2, while the other ring binds at zone 1. The size reduction from the trimethoxyphenyl ring of combretastatin A-4 to those used herein (2,5- (**129**), 3,4- (**124**), and 3,5-dimethoxyphenyl and 3-carboxy-5-aminophenyl (**84**)) are a better fit for the smaller and more polar zone 2 of the parasite orthologs. For the sulfonamides with a 6-methoxy-3-pyridyl ring, such as **320**, the pyridine ring is in zone 1. This fact confirms the importance of filling the available space in zone 2. The unoccupied space left by the smaller rings in zone 2 is responsible for the selectivity of the ligands, which are apparently associated with a affinity reduction for the host protein. The similar binding to host's and parasite's tubulin is consistent with the observed host-cell-dependent action.

The compounds stack an aromatic ring at zone 1 between Asn258β of helix H8 and the sidechain methylenes of Ser316β and Lys or Arg352β of sheets S8 and S9, respectively, making additional hydrophobic contacts along the ring plane with the sidechains of Val181α, Leu255β, Met259β, and Thr314β. The other aromatic ring is inserted edgewise towards the surface of sheets S8 and S9 boxed between the sidechains of Ser316β and Val318 (S8) or Lys or Arg352β, and Ser354β (S9). They are overlaid by helices H7 and H8 and the loop between them and interact with the sidechains of Cys241β, Leu242β, Leu248β, Ala250β, and Leu255β. These residues are highly conserved amongst the different *Leishmania* species. Therefore, the activity of the compounds might extend to other members of the genus.

4. Conclusions

A focused library of diarylsulfonamides has been designed to target the colchicine site of leishmanial but not mammalian tubulin, based on known structure-activity relationships (SAR), on the differences in amino acids between the two organisms, and the presumed favorable cost, stability, and solubility profiles. 350 new sulfonamides have been

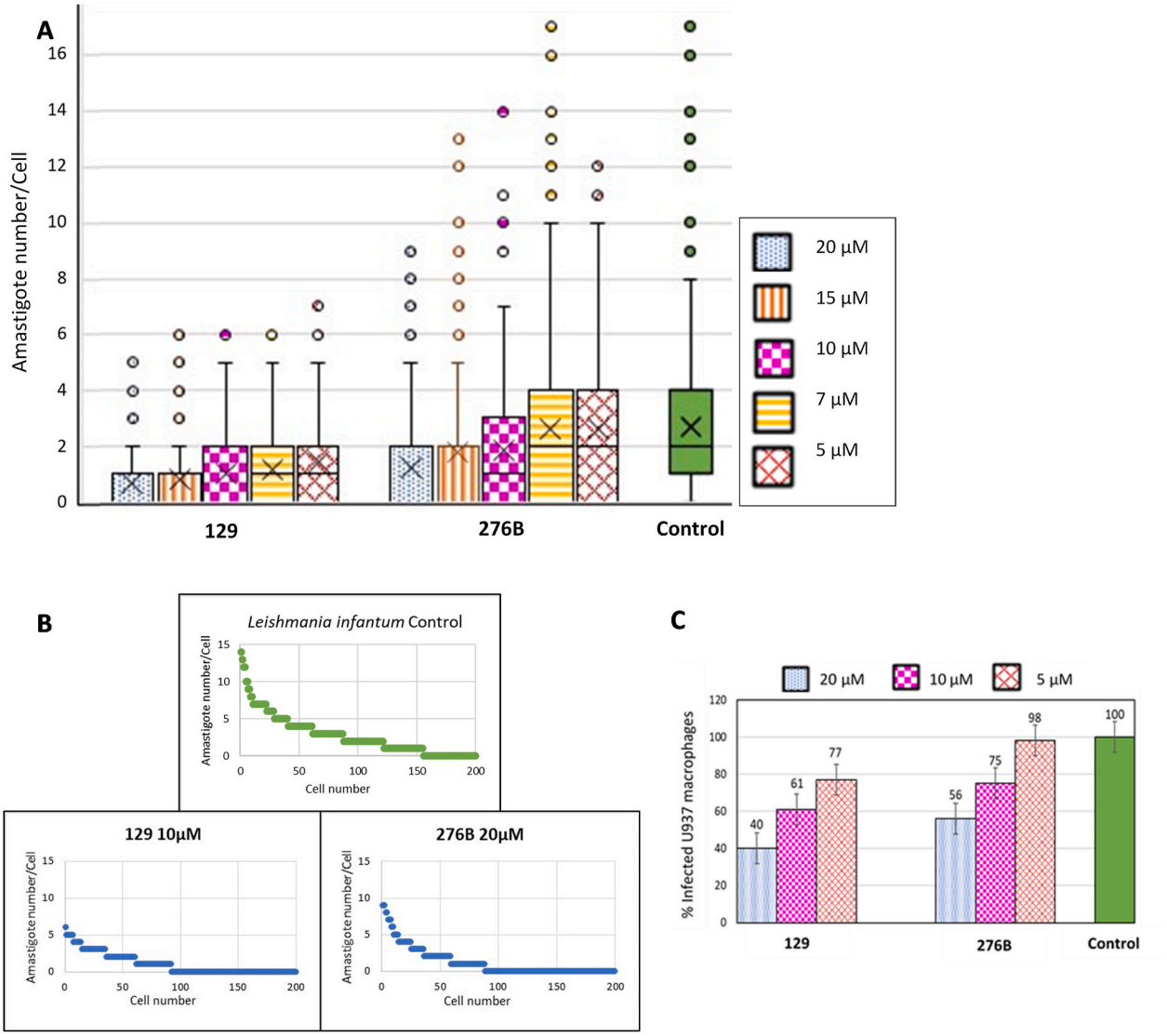

Fig. 4. Dose-response study against *L. infantum* intracellular amastigotes of non-cytotoxic sulfonamides with axenic activity. (**A**) Intracellular amastigote number per infected macrophage in the range of concentrations 20-5 µM of non-cytotoxic compounds that showed activity against both, axenic and intracellular *L. infantum* amastigotes, **129** and **276B**. Untreated control cells were run in parallel. Results shown by Box Plot data analysis are representative of three independent experiments. (**B**) Number of amastigotes accommodated per counted macrophage sorted in decreasing order in a representative sample of 200 macrophages for untreated sample (control), **129** and **276B** treatments. (**C**) Percentage of infected U937 macrophages treated with sulfonamides **129** or **276B** in a 20-5 µM concentration range normalized to the percentage of infected macrophages in untreated controls (usually about 70%), taken as 100%.

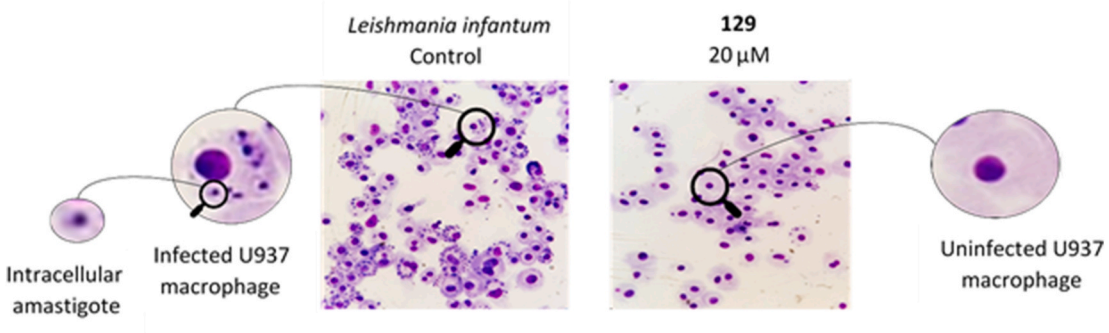

Fig. 5. Light microscopy image of modified Giemsa-stained preparations of *in vitro* macrophage infections. Left: control cells without treatment, U937 macrophages infected with *L. infantum* amastigotes. Right: Treated cells with the compound **129** at 20 µM, infection clearly interrupted.

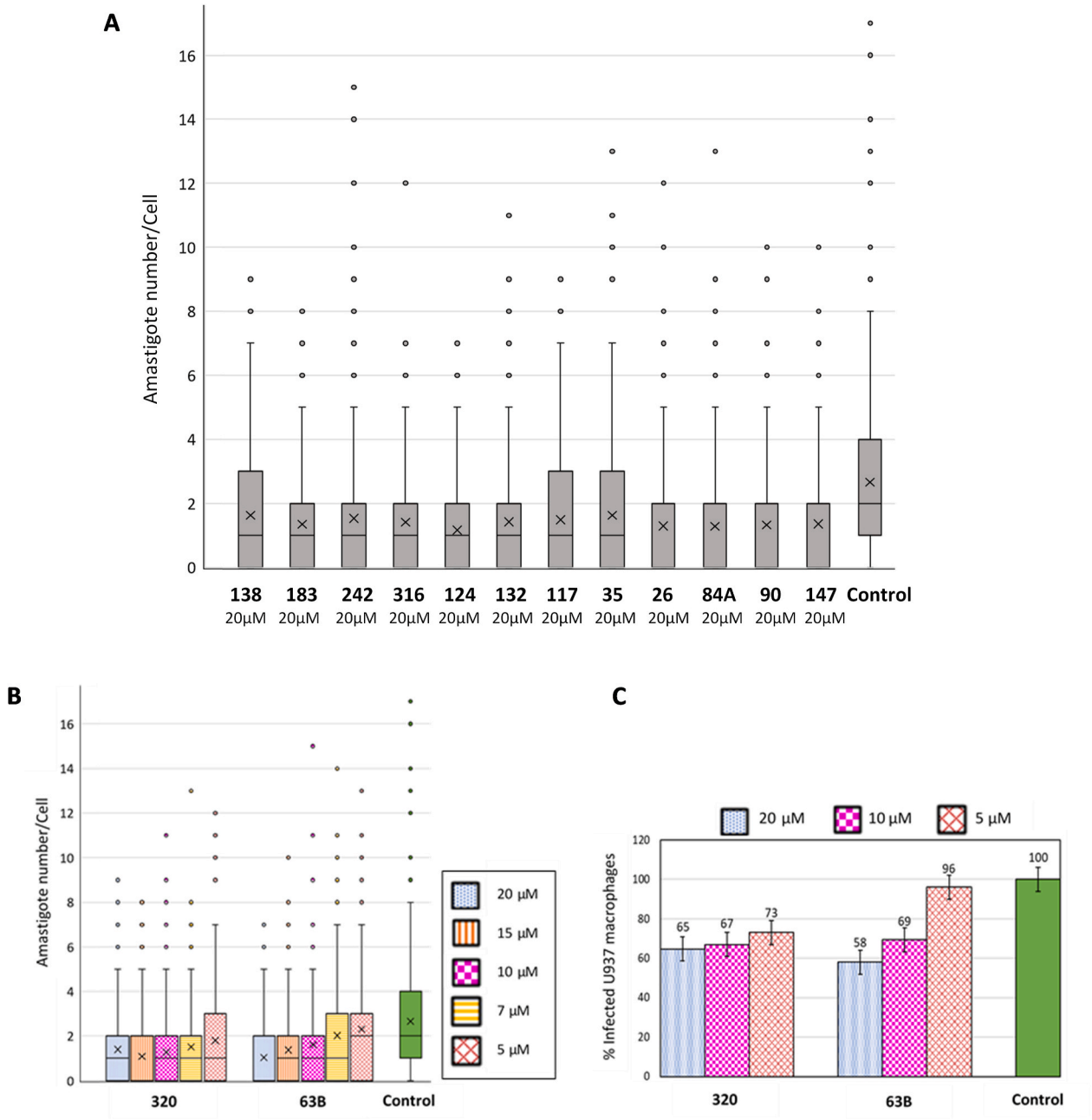

Fig. 6. Dose-response study against *L. infantum* intracellular amastigotes of non-cytotoxic sulfonamides without axenic activity. (**A**) Effect on the *L. infantum* intracellular amastigotes activity in cells treated with non-cytotoxic and non-active sulfonamides on axenic amastigotes at 10 μM, but which showed a significant *in vitro* infection decrease at 20 μM. Depicted data are representative of three independent experiments. (**B**) Box Plot data analysis of the number of intracellular amastigotes per infected cell in the 20-5 μM range of most potent non-cytotoxic sulfonamides without axenic activity that were more deeply studied, **320** and **63B**. (**C**) Percentage of infected treated cells normalized to the percentage of infected macrophages in untreated controls (usually about 70% and taken as 100%), at 20, 10, and 5 μM of compounds **320** and **63B**.

synthesized, characterized, and shown to have adequate solubility, stability, and cost compared with current antileishmanial treatments. A compound library was evaluated *in vitro* against different parasite life cycle stages using a human host cell line, leading to new compounds against the ZVL-causing agent *L. infantum*. None showed activity against promastigotes. However, eight sulfonamides (**129, 204, 332, 326B, 275, 279, 334,** and **276B**) are active against axenic amastigotes. The IC_{50} values are comprised between 0.9 and 12 μM, similar or even better than the reference drug miltefosine. The structural requirements for activity against axenic amastigotes include dimethoxyphenyl rings substituted at the 2,5-, 2,3- or 3,4-position. These requirements are not very different from those for interaction with human tubulin because 50% are also cytotoxic against cancer human cell lines. 157 compounds lacking cytotoxic activity were assayed in intracellular amastigotes. As a result, 16 severely reduced the number of axenic amastigotes found in treated infected macrophages compared to the untreated controls. The high success rate of 10% validates the design approach in a phenotypic assay reproducing the clinically relevant form in the mammalian host. Sulfonamides **129** and **276B** efficiently interrupted the course of the U937 macrophage infection in the micromolar range. These compounds constitute an starting point for development of new antileishmanial drugs. Their target is different from those of drugs under clinical trials or already implemented in clinical practice. Hence, combination therapies might be favorable. 14 of the 16 new sulfonamides active against

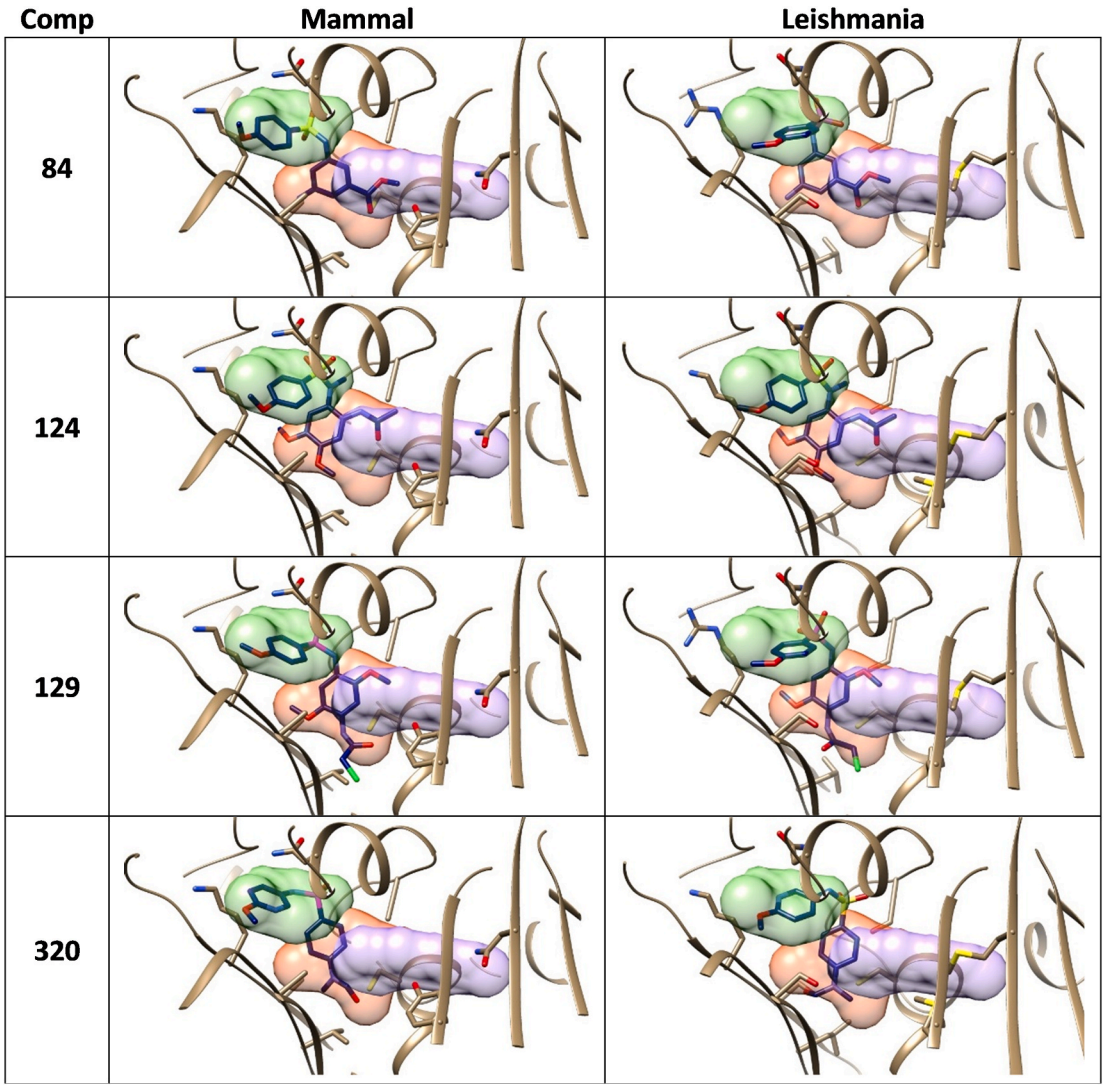

Fig. 7. Docking poses for compounds 84, 124, 129, and 320. The left column corresponds to docking in the colchicine-site of mammalian proteins and the right column to homology models for the *Leishmania* orthologs. The proteins are shown as gray cartoons. Relevant amino acid sidechains and the ligands are shown as sticks. The three zones of the colchicine-binding site are indicated as volumes colored in the same way as Fig. 1.

intracellular amastigotes lacked activity against axenic amastigotes, thus indicating a host-dependent mechanism of action devoid of toxicity which could be an advantage as an added barrier to the development of resistance by the parasite. The consistency of the biological activity found is reinforced by clustering of the active compounds in five chemical classes that also provide preliminary structure-activity relationships for further development. Molecular docking experiments support binding to the colchicine site of tubulin of the parasites, provide good agreement with the structure-activity relationship trends and suggest that the activity might extend to other *Leishmania* species. The appropriate combination of accessibility, antileishmanial activity, mechanism, parasite selectivity, and favorable solubility properties make the herein presented sulfonamides promising. The next step in development is proof-of-concept assays using animal models.

Declaration of competing interest

All authors declare no conflict of interest.

Acknowledgments

This work was supported by Consejería de Educación de la Junta de Castilla y León (SA030U16 and SA262P189) and the Spanish Ministry of Science, Innovation and Universities (RTI2018-099474-BI00) co-funded by the EU's European Regional Development Fund-FEDER, the EUROLISH NET project (Marie Sklodowska Curie ITN-ETN, EU H2020) and Fundación Ramón Areces (2017–2019). MG acknowledges a predoctoral grant EDU/602/2016 from Consejería de Educación de la Junta de Castilla y León.

Appendix A. Supplementary data

Supplementary data to this article can be found online at https://doi.org/10.1016/j.ijpddr.2021.02.006.

References

Abu Ammar, A., Nasereddin, A., Ereqat, S., Dan-Goor, M., Jaffe, C.L., Zussman, E., Abdeen, Z., 2019. Amphotericin B-loaded nanoparticles for local treatment of cutaneous leishmaniasis. Drug Deliv. Transl. Res. 9, 76–84. https://doi.org/10.1007/s13346-018-00603-0.

Alcolea, P.J., Alonso, A., Gómez, M.J., Moreno, I., Domínguez, M., Parro, V., Larraga, V., 2010. Transcriptomics throughout the life cycle of Leishmania infantum: high down-regulation rate in the amastigote stage. Int. J. Parasitol. 40, 1497–1516. https://doi.org/10.1016/j.ijpara.2010.05.013.

Alcolea, P.J., Alonso, A., Gómez, M.J., Postigo, M., Molina, R., Jiménez, M., Larraga, V., 2014. Stage-specific differential gene expression in Leishmania infantum: from the foregut of Phlebotomus perniciosus to the human phagocyte. BMC Genom. 15 https://doi.org/10.1186/1471-2164-15-849.

Alcolea, P.J., Tuñón, G.I.L., Alonso, A., García-Tabares, F., Ciordia, S., Mena, M.C., Campos, R.N.S., Almeida, R.P., Larraga, V., 2016. Differential protein abundance in promastigotes of nitric oxide-sensitive and resistant Leishmania chagasi strains. Proteonomics Clin. Appl. 10, 1132–1146. https://doi.org/10.1002/prca.201600054.

Almeida, R., Gilmartin, B.J., McCann, S.H., Norrish, A., Ivens, A.C., Lawson, D., Levick, M.P., Smith, D.F., Dyall, S.D., Vetrie, D., Freeman, T.C., Coulson, R.M., Sampaio, I., Schneider, H., Blackwell, J.M., 2004. Expression profiling of the Leishmania life cycle: cDNA arrays identify developmentally regulated genes present but not annotated in the genome. Mol. Biochem. Parasitol. 136, 87–100. https://doi.org/10.1016/j.molbiopara.2004.03.004.

Alvar, J., Vélez, I.D., Bern, C., Herrero, M., Desjeux, P., Cano, J., Jannin, J., de Boer, M., 2012. Leishmaniasis worldwide and global estimates of its incidence. PloS One. https://doi.org/10.1371/journal.pone.0035671.

Álvarez, R., Puebla, P., Díaz, J.F., Bento, A.C., García-Navas, R., De La Iglesia-Vicente, J., Mollinedo, F., Andreu, J.M., Medarde, M., Peláez, R., 2013. Endowing indole-based tubulin inhibitors with an anchor for derivatization: highly potent 3-substituted indolephenstatins and indoleisocombretastatins. J. Med. Chem. 56, 2813–2827. https://doi.org/10.1021/jm3015603.

Alves, F., Bilbe, G., Blesson, S., Goyal, V., Monnerat, S., Mowbray, C., Muthoni Ouattara, G., Pécoul, B., Rijal, S., Rode, J., Solomos, A., Strub-Wourgaft, N., Wasunna, M., Wells, S., Zijlstra, E.E., Arana, B., Alvar, J., 2018. Recent development of visceral leishmaniasis treatments: successes, pitfalls, and perspectives. Clin. Microbiol. Rev. https://doi.org/10.1128/CMR.00048-18.

Arce, A., Estirado, A., Ordobas, M., Sevilla, S., García, N., Moratilla, L., de la Fuente, S., Martínez, A.M., Pérez, A.M., Aránguez, E., Iriso, A., Sevillano, O., Bernal, J., Vilas, F., 2013. Re-emergence of Leishmaniasis in Spain: Community Outbreak in Madrid, Spain, 2009 TO 2012. https://doi.org/10.2807/1560-7917.ES2013.18.30.20546. Eurosurveillance 18.

Bateman, A., 2019. UniProt: a worldwide hub of protein knowledge. Nucleic Acids Res. 47, D506–D515. https://doi.org/10.1093/nar/gky1049.

Berman, H., Henrick, K., Nakamura, H., 2003. Announcing the worldwide protein Data Bank. Nat. Struct. Biol. https://doi.org/10.1038/nsb1203-980.

Berthold, M.R., Cebron, N., Dill, F., Gabriel, T.R., Kötter, T., Meinl, T., Ohl, P., Sieb, C., Thiel, K., Wiswedel, B., 2007. KNIME: the konstanz information miner. Studies in Classification, Data Analysis, and Knowledge Organization. Springer Berlin, Ger, pp. 319–326.

Daina, A., Michielin, O., Zoete, V., 2017. SwissADME: a free web tool to evaluate pharmacokinetics, drug-likeness and medicinal chemistry friendliness of small molecules. Sci. Rep. 7 https://doi.org/10.1038/srep42717.

De Muylder, G., Ang, K.K.H., Chen, S., Arkin, M.R., Engel, J.C., McKerrow, J.H., 2011. A screen against leishmania intracellular amastigotes: comparison to a promastigote screen and identification of a host cell-specific hit. PLoS Neglected Trop. Dis. 5 https://doi.org/10.1371/journal.pntd.0001253.

De Rycker, M., Baragaña, B., Duce, S.L., Gilbert, I.H., 2018. Challenges and recent progress in drug discovery for tropical diseases. Nature. https://doi.org/10.1038/s41586-018-0327-4.

Dostál, V., Libusová, L., 2014. Microtubule Drugs: Action, Selectivity, and Resistance across the Kingdoms of Life. Protoplasma. https://doi.org/10.1007/s00709-014-0633-0.

Drews, J., 2000. Drug discovery: a historical perspective. Science 80–. https://doi.org/10.1126/science.287.5460.1960.

Dumontet, C., Jordan, M.A., 2010. Microtubule-binding agents: a dynamic field of cancer therapeutics. Nat. Rev. Drug Discov. https://doi.org/10.1038/nrd3253.

Escudero-Martínez, J.M., Pérez-Pertejo, Y., Reguera, R.M., Castro, M.Á., Rojo, M.V., Santiago, C., Abad, A., García, P.A., López-Pérez, J.L., San Feliciano, A., Balaña-Fouce, R., 2017. Antileishmanial activity and tubulin polymerization inhibition of podophyllotoxin derivatives on Leishmania infantum. Int. J. Parasitol. Drugs Drug Resist. 7, 272–285. https://doi.org/10.1016/j.ijpddr.2017.06.003.

Forli, S., Huey, R., Pique, M.E., Sanner, M.F., Goodsell, D.S., Olson, A.J., 2016. Computational protein-ligand docking and virtual drug screening with the AutoDock suite. Nat. Protoc. 11, 905–919. https://doi.org/10.1038/nprot.2016.051.

Furtado, L.F.V., de Paiva Bello, A.C.P., Rabelo, É.M.L., 2016. Benzimidazole resistance in helminths: from problem to diagnosis. Acta Trop. https://doi.org/10.1016/j.actatropica.2016.06.021.

Garcia-Perez, C., Pelaez, R., Theron, R., Luis Lopez-Perez, J., 2017. JADOPPT: java based AutoDock preparing and processing tool. Bioinformatics 33, 583–585. https://doi.org/10.1093/bioinformatics/btw677.

Jain, V., Jain, K., 2018. Molecular targets and pathways for the treatment of visceral leishmaniasis. Drug Discov. Today. https://doi.org/10.1016/j.drudis.2017.09.006.

Jiménez, M., González, E., Martín-Martín, I., Hernández, S., Molina, R., 2014. Could wild rabbits (Oryctolagus cuniculus) be reservoirs for Leishmania infantum in the focus of Madrid, Spain? Vet. Parasitol. 202, 296–300. https://doi.org/10.1016/j.vetpar.2014.03.027.

Jordan, A., Hadfield, J.A., Lawrence, N.J., McGown, A.T., 1998. Tubulin as a target for anticancer drugs: agents which interact with the mitotic spindle. Med. Res. Rev. 18, 259–296. https://doi.org/10.1002/(SICI)1098-1128.

Korb, O., Stützle, T., Exner, T.E., 2009. Empirical scoring functions for advanced Protein-Ligand docking with PLANTS. J. Chem. Inf. Model. 49, 84–96. https://doi.org/10.1021/ci800298z.

Lacey, E., 1990. Mode of action of benzimidazoles. Parasitol. Today 6, 112–115. https://doi.org/10.1016/0169-4758(90)90227-U.

Larkin, M.A., Blackshields, G., Brown, N.P., Chenna, R., Mcgettigan, P.A., McWilliam, H., Valentin, F., Wallace, I.M., Wilm, A., Lopez, R., Thompson, J.D., Gibson, T.J., Higgins, D.G., 2007. Clustal W and clustal X version 2.0. Bioinformatics 23, 2947–2948. https://doi.org/10.1093/bioinformatics/btm404.

Laurence, C., Brameld, K.A., Graton, J., Le Questel, J.Y., Renault, E., 2009. The pKBHX database: toward a better understanding of hydrogen-bond basicity for medicinal chemists. J. Med. Chem. https://doi.org/10.1021/jm801331y.

Légaré, D., Richard, D., Mukhopadhyay, R., Stierhof, Y.D., Rosen, B.P., Haimeur, A., Papadopoulou, B., Ouellette, M., 2001. The leishmania ATP-binding cassette protein PGPA is an intracellular metal-thiol transporter ATPase. J. Biol. Chem. 276, 26301–26307. https://doi.org/10.1074/jbc.M102351200.

Leifso, K., Cohen-Freue, G., Dogra, N., Murray, A., McMaster, W.R., 2007. Genomic and proteomic expression analysis of Leishmania promastigote and amastigote life stages: the Leishmania genome is constitutively expressed. Mol. Biochem. Parasitol. 152, 35–46. https://doi.org/10.1016/j.molbiopara.2006.11.009.

Luis, L., Serrano, M.L., Hidalgo, M., Mendoza-León, A., 2013. Comparative analyses of the β-tubulin gene and molecular modeling reveal molecular insight into the colchicine resistance in kinetoplastids organisms. BioMed Res. Int. 843748. https://doi.org/10.1155/2013/843748.

Marquis, N., Gourbal, B., Rosen, B.P., Mukhopadhyay, R., Ouellette, M., 2005. Modulation in aquaglyceroporin AQP1 gene transcript levels in drug-resistant Leishmania. Mol. Microbiol. 57, 1690–1699. https://doi.org/10.1111/j.1365-2958.2005.04782.x.

Marvin, 2017. ChemAxon [WWW Document]. URL, vol. 8. accessed 5.2.20. https://www.chemaxon.com.

Massarotti, A., Coluccia, A., Silvestri, R., Sorba, G., Brancale, A., 2012. The tubulin colchicine domain: a molecular modeling perspective. ChemMedChem. https://doi.org/10.1002/cmdc.201100361.

Mbongo, N., Loiseau, P.M., Billion, M.A., Robert-Gero, M., 1998. Mechanism of amphotericin B resistance in Leishmania donovani promastigotes. Antimicrob. Agents Chemother. 42, 352–357. https://doi.org/10.1128/AAC.00030-11.

Molina, R., Jiménez, M.I., Cruz, I., Iriso, A., Martín-Martín, I., Sevillano, O., Melero, S., Bernal, J., 2012. The hare (Lepus granatensis) as potential sylvatic reservoir of Leishmania infantum in Spain. Vet. Parasitol. 190, 268–271. https://doi.org/10.1016/j.vetpar.2012.05.006.

Mondelaers, A., Sanchez-Cañete, M.P., Hendrickx, S., Eberhardt, E., Garcia-Hernandez, R., Lachaud, L., Cotton, J., Sanders, M., Cuypers, B., Imamura, H., Dujardin, J.-C., Delputte, P., Cos, P., Caljon, G., Gamarro, F., Castanys, S., Maes, L., 2016. Genomic and molecular characterization of miltefosine resistance in leishmania infantum strains with either natural or acquired resistance through experimental selection of intracellular amastigotes. PloS One 11, e0154101. https://doi.org/10.1371/journal.pone.0154101.

Montecinos-Franjola, F., Chaturvedi, S.K., Schuck, P., Sackett, D.L., 2019. All tubulins are not alike: heterodimer dissociation differs among different biological sources. J. Biol. Chem. 294, 10315–10324. https://doi.org/10.1074/jbc.RA119.007973.

Monzote, L., 2009. Current treatment of leishmaniasis: a review. Open Antimicrob. Agents J. https://doi.org/10.2174/1874518100901010009.

Nagle, A.S., Khare, S., Kumar, A.B., Supek, F., Buchynskyy, A., Mathison, C.J.N., Chennamaneni, N.K., Pendem, N., Buckner, F.S., Gelb, M.H., Molteni, V., 2014. Recent developments in drug discovery for leishmaniasis and human african trypanosomiasis. Chem. Rev. https://doi.org/10.1021/cr500365f.

OpenEye Scientific Software, 2019. [WWW Document]. URL. Inc, Santa Fe. accessed 5.2.20. https://www.eyesopen.com/.

Pérez-Victoria, F.J., Gamarro, F., Ouellette, M., Castanys, S., 2003. Functional cloning of the miltefosine transporter: a novel p-type phospholipid translocase from leishmania involved in drug resistance. J. Biol. Chem. 278, 49965–49971. https://doi.org/10.1074/jbc.M308352200.

Pérez-Victoria, F.J., Sánchez-Cañete, M.P., Seifert, K., Croft, S.L., Sundar, S., Castanys, S., Gamarro, F., 2006. Mechanisms of experimental resistance of Leishmania to miltefosine: implications for clinical use. Drug Resist. Updates 9, 26–39. https://doi.org/10.1016/j.drup.2006.04.001.

Perlovich, G.L., Kazachenko, V.P., Strakhova, N.N., Raevsky, O.A., 2014. Impact of sulfonamide structure on solubility and transfer processes in biologically relevant solvents. J. Chem. Eng. Data 59, 4217–4226. https://doi.org/10.1021/je500918t.

Pettersen, E.F., Goddard, T.D., Huang, C.C., Couch, G.S., Greenblatt, D.M., Meng, E.C., Ferrin, T.E., 2004. UCSF Chimera-A visualization system for exploratory research and analysis. J. Comput. Chem. 25, 1605–1612. https://doi.org/10.1002/jcc.20084.

Ponte-Sucre, A., Gamarro, F., Dujardin, J.C., Barrett, M.P., López-Vélez, R., García-Hernández, R., Pountain, A.W., Mwenechanya, R., Papadopoulou, B., 2017. Drug resistance and treatment failure in leishmaniasis: a 21st century challenge. PLoS Neglected Trop. Dis. https://doi.org/10.1371/journal.pntd.0006052.

Rama, M., Kumar, N.V., enkates, A., Balaji, S., 2015. A comprehensive review of patented antileishmanial agents. Pharm. Pat. Anal. https://doi.org/10.4155/ppa.14.55.

Rijal, S., Ostyn, B., Uranw, S., Rai, K., Bhattarai, N.R., Dorlo, T.P.C., Beijnen, J.H., Vanaerschot, M., Decuypere, S., Dhakal, S.S., Das, M.L., Karki, P., Singh, R., Boelaert, M., Dujardin, J.-C., 2013. Increasing failure of miltefosine in the treatment of Kala-azar in Nepal and the potential role of parasite drug resistance, reinfection, or noncompliance. Clin. Infect. Dis. 56, 1530–1538. https://doi.org/10.1093/cid/cit102.

Rochette, A., Raymond, F., Corbeil, J., Ouellette, M., Papadopoulou, B., 2009. Whole-genome comparative RNA expression profiling of axenic and intracellular amastigote forms of Leishmania infantum. Mol. Biochem. Parasitol. 165, 32–47. https://doi.org/10.1016/j.molbiopara.2008.12.012.

Šali, A., Blundell, T.L., 1993. Comparative protein modelling by satisfaction of spatial restraints. J. Mol. Biol. 234, 779–815. https://doi.org/10.1006/jmbi.1993.1626.

Scudiero, D.A., Shoemaker, R.H., Paull, K.D., Monks, A., Tierney, S., Nofziger, T.H., Currens, M.J., Seniff, D., Boyd, M.R., 1988. Evaluation of a soluble tetrazolium/formazan assay for cell growth and drug sensitivity in culture using human and other tumor cell lines. Canc. Res. 48, 4827–4833.

Sinclair, A.N., de Graffenried, C.L., 2019. More than microtubules: the structure and function of the subpellicular array in trypanosomatids. Trends Parasitol. https://doi.org/10.1016/j.pt.2019.07.008.

Sundar, S., Jha, T.K., Thakur, C.P., Engel, J., Sindermann, H., Fischer, C., Junge, K., Bryceson, A., Berman, J., 2002. Oral miltefosine for Indian visceral leishmaniasis. N. Engl. J. Med. 347, 1739–1746. https://doi.org/10.1056/NEJMoa021556.

Sundar, S., Jha, T.K., Thakur, C.P., Sinha, P.K., Bhattacharya, S.K., 2007. Injectable paromomycin for visceral leishmaniasis in India. N. Engl. J. Med. 356, 2571–2581. https://doi.org/10.1056/NEJMoa066536.

Sundar, S., Murray, H.W., 2005. Availability of miltefosine for the treatment of kala-azar in India. Bull. World Health Organ. 83, 394–395. https://doi.org/10.1590/S0042-96862005000500018.

Sunter, J., Gull, K., 2017. Shape, form, function and Leishmania pathogenicity: from textbook descriptions to biological understanding. Open Biol. https://doi.org/10.1098/rsob.170165.

Tiuman, T.S., Santos, A.O., Ueda-Nakamura, T., Filho, B.P.D., Nakamura, C.V., 2011. Recent advances in leishmaniasis treatment. Int. J. Infect. Dis. https://doi.org/10.1016/j.ijid.2011.03.021.

Vandermeulen, G., Rouxhet, L., Arien, A., Brewster, M.E., Préat, V., 2006. Encapsulation of amphotericin B in poly(ethylene glycol)-block-poly(ε- caprolactone-co-trimethylenecarbonate) polymeric micelles. Int. J. Pharm. 309, 234–240. https://doi.org/10.1016/j.ijpharm.2005.11.031.

Vicente-Blázquez, A., González, M., Álvarez, R., del Mazo, S., Medarde, M., Peláez, R., 2019. Antitubulin sulfonamides: the successful combination of an established drug class and a multifaceted target. Med. Res. Rev. 39, 775–830. https://doi.org/10.1002/med.21541.

Zhang, C., Bourgeade Delmas, S., Fernández Álvarez, Á., Valentin, A., Hemmert, C., Gornitzka, H., 2018. Synthesis, characterization, and antileishmanial activity of neutral N-heterocyclic carbenes gold(I) complexes. Eur. J. Med. Chem. 143, 1635–1643. https://doi.org/10.1016/j.ejmech.2017.10.060.

Zulfiqar, B., Shelper, T.B., Avery, V.M., 2017. Leishmaniasis drug discovery: recent progress and challenges in assay development. Drug Discov. Today. https://doi.org/10.1016/j.drudis.2017.06.004.